2.2. Biochemical analyses

Plasma glucose was measured by the glucose oxidase method, and hemoglobin A_{1c} (HbA_{1c}) was measured by a high-performance liquid chromatography method. Serum insulin level was measured using commercial radioimmunoassay kits (Shionogi, Osaka, Japan). Serum leptin level was determined by radioimmunoassay using commercial kits (Linco Research, St Charles, MO). Serum adiponectin level was determined by radioimmunoassay using commercial kits (Otsuka assay, Osaka, Japan) [6].

2.3. Oral glucose tolerance test

A standard oral glucose tolerance test (OGTT) with 75 g of glucose was performed after a 12-hour overnight fast. Venous blood was collected for determination of glucose and insulin concentrations immediately before glucose administration and at 30-minute intervals thereafter for 120 minutes.

2.4. Magnetic resonance imaging technique

Magnetic resonance imaging (MRI) was performed using a 1.5-T imaging device (Sigma Horizon; General Electric, Milwaukee, WI). The upper and lower limbs were surveyed using contiguous axial, 10-mm slices. Fat was easily identified on MRI because of its short T1 relaxation time and its relatively high signal intensity on images compared with other tissues such as muscle.

2.5. Dual-energy x-ray absorptiometry

Whole-body DEXA scan was performed with a multiple detector fan-beam Hologic (Bedford, MA) QDR-4500W densitometer. Data were obtained from the head, upper extremities, trunk, and lower extremities. Proportions of fat in individual regions as well as the whole body were calculated as percentage of body mass. Data were also obtained for measurement of lean tissue mass and bone mineral density.

2.6. Measurement of fat distribution

Subcutaneous and visceral fat distributions were determined by measuring a −150- to −50-Hounsfield unit area using a modification of the method of computed tomographic (CT) scanning (Light Speed Plus-R, General Electric) by Tokunaga et al at the umbilical level [7]. Computed tomographic images were obtained both at baseline and after 9 months of treatment. The V/S ratio was calculated as visceral adipose tissue area divided by subcutaneous adipose tissue area.

2.7. Sequence analyses

Sequence analyses of *LMNA* and *PPARG* were performed in the patient. The patient gave written informed consent for all genetic analyses, which were approved by the Ethical Committee of Kyoto University Graduate School of Medicine. Genomic DNA was isolated from blood using an InstaGene Whole Blood kit (Bio-Rad, Hercules, CA) according to the manufacturer's protocol. Polymerase chain reaction primers, including exon-specific fragments and splice sites, were designed using genomic DNA sequences of human *LMNA* and *PPARG* obtained from GenBank accession numbers NM-170707, AB005520, and AB005526, respectively, as well as published sequences [8,9]. Polymerase chain reaction products were separated by electrophoresis in a 2% agarose gel, purified, and sequenced directly by the chain termination method with both forward and reverse primers on an ABI PRISM310 Genetic Analyzer (PerkinElmer, PE Applied Biosystems, Foster City, CA). All exons and intron-exon boundaries of *AKT2* were amplified and sequenced using primers as previously described [10]. The exons and intron-exon boundaries of caveolin-1 were amplified and bidirectionally sequenced using primers and conditions as previously described [11]. A previously reported method was used to detect the *PPARG4* promoter mutation [12].

3. Case report

The patient is a 46-year-old woman. When she was 34 years old, a diagnosis of diabetes was made by a family physician on the basis of HbA_{1c} and high postprandial glucose levels. However, she decided not to receive any medications for diabetes. She was introduced to our hospital for treatment in December 1998 because of poor glycemic control at 40 years of age. She had a body mass index (BMI) of 23 (height, 160 cm; body weight, 58.5 kg). She had no history of hypertension or autoimmune disease. She was premenopausal status. There was no evidence of axial acanthosis nigricans. In January 1999, HbA_{1c} was 11.6% and her lipid profile was normal (Table 1). An OGTT was performed in September 1999, when she was receiving 10 mg of glibenclamide and 0.6 mg of voglibose and her HbA_{1c} was 8.2%. As shown in Table 2, the insulin levels during OGTT were relatively high, suggesting mild insulin resistance. When serum leptin and adiponectin were measured before her second pioglitazone treatment, she had a BMI of 25.3. Her serum leptin level was 10.4 ng/

Table 1
Biochemical data for this patient

Metabolic variables	Patient
Plasma glucose (mg/dL)	245
HbA_{1c} (%)	11.6
Plasma insulin (μU/mL)	19.1
Serum triglycerides (mg/dL)	137
Serum cholesterol (mg/dL)	200
Serum HDL cholesterol (mg/dL)	49
Serum leptin (ng/mL)	10.4
Serum adiponectin (μg/mL)	3.5

All samples were obtained after a 12-hour overnight fast. HDL indicates high-density lipoprotein.

Table 2
Plasma glucose and insulin levels before and 30, 60, and 120 minutes after an oral 75-g glucose load

	Time (min)			
	0	30	60	120
Plasma glucose (mg/dL)	245	342	409	401
Plasma insulin (μU/mL)	17.7	31.3	79.7	33.0

mL, whereas her serum adiponectin was 3.5 μg/mL (Table 1). An abdominal ultrasound examination revealed hepatic steatosis (unpresented data). She had first noted her decreased subcutaneous fat over her lower limbs at 12 years of age. As shown in Fig. 1B, she exhibited loss of fat in subcutaneous deposits in the lower limbs and buttocks, with prominent lower limbs musculature and excess fat deposition around the face, neck, and trunk. As shown in Fig. 1A, her mother and 2 sisters had a similar physical appearance; and an autosomal dominant pattern of inheritance was therefore considered. A clinical diagnosis of FPLD was therefore made. Her mother had diet-controlled diabetes diagnosed at 75 years of age and died of cerebral infarction at 80 years old. Her father, son, and daughter each had neither fat atrophy nor diabetes mellitus. Her father died of lung cancer at 64 years of age. As shown in Fig. 2, we began initial combined treatment with pioglitazone and insulin injection for diabetes in March 2000, but discontinued pioglitazone in March 2001 because of weight gain. After approximately 3-year washout of pioglitazone, we noted fat atrophy over her lower limbs and assessed body fat distribution by DEXA, MRI, and CT studies in March 2004. As shown in Fig. 1C, T1-weighed MR images at the level of the gluteal fat revealed the striking loss of gluteal subcutaneous fat. As shown in Fig. 1D, axial MRI at the level of the thigh and calf in the patient revealed nearly complete absence of subcutaneous fat in the thigh and calf. As shown in Fig. 1E, axial T1 MRI at the level of the arm and forearm in the patient revealed the preservation of subcutaneous fat. As shown in Fig. 1F, thoracic and abdominal CT revealed preservation of subcutaneous fat in the abdominal and thoracic regions. Table 3 shows the regional and whole-body adipose tissue distribution and body composition estimated by DEXA scan. Compared with healthy subjects, she had markedly decreased fat in her legs, with prominent accumulation in the trunk. Fat accumulation was preserved in her upper limbs. She appeared to have well-preserved skeletal muscle mass.

The first pioglitazone treatment was performed before the diagnosis of FPLD and was markedly effective in improving glycemic control.

Glibenclamide (2.5 mg) and voglibose 0.6 mg/d were started in December 1998; and although the dose of glibenclamide was increased to 10 mg/d, her HbA_{1c} was 9.5% and remained high. Injection of biphasic human insulin (BHI 30) was added at a dose of 16 U/d, and the dose of insulin was increased to 30 U/d; but HbA_{1c} was still 8.0%, and her blood glucose level remained unsatisfactory. Her body weight gain was about 3 kg, and BMI was increased to 24.4 during combined treatment with glibenclamide and insulin. We stopped the glibenclamide and prescribed metformin 500 mg/d, but HbA_{1c} increased to 11.2%. We therefore discontinued the metformin and initiated combined treatment with pioglitazone (30 mg/d) and insulin in March 2000. Her response to pioglitazone was monitored by HbA_{1c}. Fig. 2 shows HbA_{1c} level during treatment. Decline in HbA_{1c} was observed at 2 months; and the decrease continued to be observed throughout the treatment, with lowest values at 6 months. After 6 months of treatment, HbA_{1c} had decreased from 11.2% to 6.1% and remained thereafter at about 6.0%. After 7 months of treatment, the dose of insulin was decreased to 20 U/d. Fig. 2 also shows change in body weight during treatment. After 12 months, body weight had increased from 62.0 to 71.0 kg. We stopped pioglitazone in March 2001 because of this weight gain.

3.1. Changes in body fat distribution and serum adiponectin during the second pioglitazone treatment

About 3 years had passed since she received the combined treatment with 4 mg glimepiride and 30 U/d insulin injection (BHI 30) instead of pioglitazone. Her blood glucose level remained unsatisfactory. We therefore began administration of a half-dose (15 mg) of pioglitazone in April 2004 to prevent body weight gain. Change in fat and lean mass was monitored during pioglitazone treatment by DEXA scan. We also evaluated changes in subcutaneous and visceral fat area by abdominal CT and adiponectin level during pioglitazone treatment. After 9 months of treatment, HbA_{1c} level was reduced from 8.5% to 6.2% and remained stable thereafter, whereas body weight increased by about 3 kg (Fig. 3). As shown in Table 4, comparison of DEXA scan results showed that fat mass increased by 2.2 kg, whereas lean mass increased by 0.7 kg during pioglitazone treatment. Pioglitazone induced increase in fat mass almost equally in the upper limbs, lower limbs, and trunk, although the increase was slightly less in the lower limbs than in the other 2 regions. Interestingly, the increase in lean mass in the lower limbs was greater than that in the upper limbs and trunk, whereas the increase in lean mass in the upper limbs and trunk was suppressed. We also evaluated the accumulation of subcutaneous and visceral fat by CT scan at the umbilical levels before and after 9 months of pioglitazone treatment. Pioglitazone increased subcutaneous fat from 160.0 to 211.3 cm^2, but resulted in almost no change in visceral fat (103.7 vs 106.2 cm^2). After 9 months of treatment, serum adiponectin had increased from 3.5 to 21.7 μg/mL.

3.2. Sequence analysis

We examined the sequences of the entire coding regions and exon-intron boundary regions of the *LMNA*, *PPARG*,

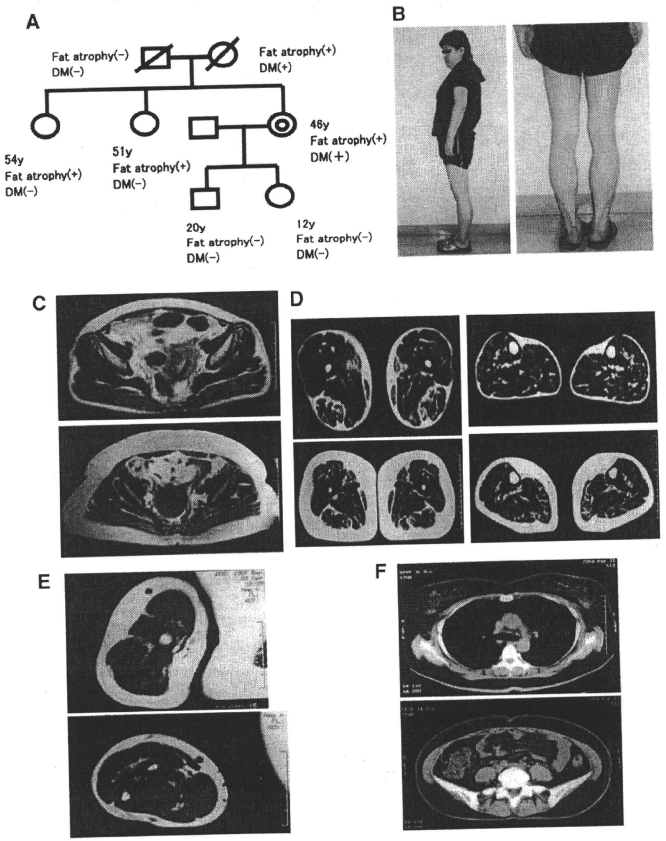

Fig. 1. A, The pedigree of a Japanese family with an unusual type of FPLD. The proband, her mother, and 2 sisters exhibited marked loss of subcutaneous fat in the lower limbs and buttocks. The proband and her mother had diabetes mellitus. B, Phenotypic features of the patient. Note the prominent lower limbs musculature as well as the preservation of abdominal and cervical fat with loss of lower limbs and gluteal fat deposits. C, T1-weighted MR images at the level of the gluteal fat indicate striking loss of gluteal subcutaneous fat in the upper panel. Control images obtained from a healthy female individual are shown in lower panel. D, T1-weighted MR images at the level of the thigh (left panel) and calf (right panel) in the patient reveal nearly complete absence of subcutaneous fat. Control images obtained from a healthy female individual are shown in the lower panel. E, T1-weighted MR images at the level of the arm (upper panel) and forearm (lower panel) in the patient indicate preservation of subcutaneous fat. F, Thoracic CT at the level of the fourth thoracic vertebrae and abdominal CT at the umbilical level. Thoracic (upper panel) and abdominal (lower panel) findings reveal that CT showed the preservation of subcutaneous fat in the abdomen and thoracic region.

AKT2, and caveolin-1 genes, but found no mutations of these genes in the proband. We also checked for −14A>G substitution upstream from exon 1 within the *PPARG4* promoter, but did not find this mutation.

4. Discussion

In this article, we have described a 46-year-old Japanese diabetic woman with an unusual type of FPLD. She has

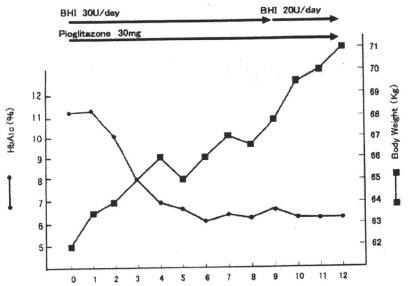

Fig. 2. Hemoglobin A_{1c} level and body weight during the first pioglitazone treatment. Pioglitazone (30 mg) was administered and dramatically improved glycemic control. However, it was stopped because of body weight gain.

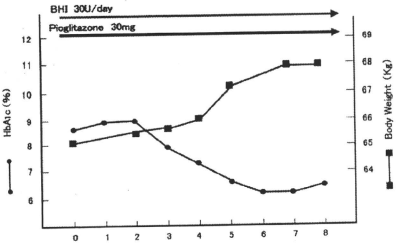

Fig. 3. Hemoglobin A_{1c} level and body weight during the second pioglitazone treatment. The dose of pioglitazone was 15 mg to prevent excessive body weight gain. Changes in body fat composition were evaluated by DEXA scan and abdominal CT as well as serum adiponectin level after 9 months of pioglitazone treatment.

marked loss of subcutaneous fat in her lower limbs and buttocks, with sparing of the face, neck, upper limbs, and trunk. The cases of FPLD reported thus far have predominantly affected the limbs and gluteal fat deposits, with variable truncal involvement but normal or excess fat on the face and neck [2,5,13-16,18-20]. The distribution of fat atrophy in the present case thus appears to be rare.

The loss of body fat in FPLD can be caused by defects in the development and/or differentiation of adipose tissue as a consequence of mutations in a number of genes, including *LMNA*, *PPARG*, *AKT2*, and caveolin-1 [2,15]. Patients with *LMNA* gene mutation have FPLD as indicated by a loss in subcutaneous fat in the upper and lower limbs [2,17]. Patients with *PPARG* gene mutation also have FPLD, as indicated by a loss of fat in subcutaneous deposits in the limbs, affecting the distal regions of the extremities such as the forearms and calves more than the proximal regions, but with preservation of visceral and abdominal subcutaneous fat [2,18-20]. It appears likely that our patient has no mutation of the *LMNA* or *PPARG* gene because she has a phenotype of lipodystrophy distinct from that of patients with *LMNA* gene or *PPARG* gene mutation.

Recently, George et al [10] reported a heterozygous missense mutation R274H in the *AKT2* gene in a family in which affected subjects developed insulin resistance, diabetes mellitus, and hypertension. The proband, a 34-year-old woman, had partial lipodystrophy affecting her extremities. Cao et al [15] also reported a heterozygous

Table 3
Body composition as determined by DEXA scan in the proband

	Proband	Mean values (in control subjects)
Height (cm)	160.0	156.1 ± 4.9
Body weight (kg)	64.0	55.1 ± 6.7
BMI (kg/m^2)	25.0	22.7 ± 3.0
Age (y)	46	45.1 ± 2.8
Fat (%)		
Whole body	33.1	30.3 ± 6.2
1 Arm	42.9	26.9 ± 7.3
1 Leg	13.0	33.2 ± 5.7
Trunk	40.4	28.4 ± 7.7
Fat mass (kg)		
Whole body	20.2	16.8 ± 5.2
1 Arm	1.3	0.7 ± 0.3
1 Leg	0.9	3.5 ± 1.0
Trunk	15.0	7.1 ± 2.8
Lean mass (kg)		
Whole body	38.8	35.3 ± 3.1
1 Arm	1.7	1.7 ± 0.2
1 Leg	5.4	6.6 ± 0.9
Trunk	21.5	16.3 ± 1.3

Normal values are obtained from 55 healthy middle-aged women. Fat, fat mass, and lean mass in 1 arm and leg indicate the mean values of left and right arm (or leg).

Table 4
Changes in fat and lean mass determined by DEXA, subcutaneous and visceral fat areas determined by abdominal CT, and serum adiponectin level during pioglitazone treatment

	Pioglitazone		
	Pre	Post	Change
Body weight (kg)	65.0	68.0	+3.0
Fat (kg)			
Whole body	20.2	22.4	+2.2
Arms	2.7	3.5	+0.8
Legs	1.7	2.2	+0.5
Trunk	15.0	15.9	+0.9
Lean mass (kg)			
Whole body	38.8	39.5	+0.7
Arms	3.3	3.1	−0.2
Legs	10.8	11.9	+1.1
Trunk	21.5	21.3	−0.2
CT (umbilical level)			
Subcutaneous fat (cm^2)	160	211.3	+51.3
Visceral (cm^2)	103.7	106.2	+2.5
Adiponectin (μg/mL)	3.5	21.7	+18.2

caveolin-1 frameshift mutation in patients with atypical partial lipodystrophy and hypertriglyceridemia. We were therefore interested in the possibility of involvement of the *AKT2* and caveolin-1 genes in this case and added mutational analysis, including *AKT2* and caveolin-1. However, we found no mutations in these genes. This case thus features an unusual phenotype, with no mutation of the causing gene in FPLD, *LMNA*, *PPARG*, *AKT2*, caveolin-1, and *PPARG4* promoter. It is thus possible that the present case is due to a defect of a novel gene. However, we could not analyze messenger RNA (mRNA) of candidate gene in this article; and we could not rule out the following possibility. The mutation might be located anywhere except the entire coding regions and exon-intron boundary regions in candidate gene. It might either cause the dysfunction of mRNA of candidate gene or, alternatively, decrease levels of mRNA of candidate gene [21].

Pioglitazone was markedly effective in improving glycemic control in our case. As shown in Fig. 2, HbA_{1c} level decreased by 5.1% in our patient after 6 months of treatment with pioglitazone. Marked weight gain was also observed in our patient during pioglitazone treatment. This observation was compatible with a previous report [14], suggesting that it may result from synergism between thiazolidinediones (TZDs) and insulin-promoting adipogenesis. The level of adiponectin was low before treatment, but increased markedly during pioglitazone treatment. Thiazolidinediones seemed ideally suited to treat lipoatrophic diabetes [22]. Almost all diabetic patients in this study had partial lipodystrophy. In the 13 patients with diabetes who completed 6 months of troglitazone treatment, HbA_{1c} levels significantly decreased by a mean of 2.8%.Troglitazone treatment significantly increased body fat without significant change in weight. Savage et al [18] reported that subject 2 (S2) with FPLD was heterozygous for a proline-467-leucine (P467L) mutation in *PPARG*, whereas subject 3 (S3) with FPLD was heterozygous for a valine-290-methionine (V290M) mutation in *PPARG*. The metabolic impact of rosiglitazone was much more striking in S2, in whom insulin sensitivity and HbA_{1c} were both normalized, whereas S3 remained severely insulin resistant and exhibited little change in HbA_{1c}. Fat mass was increased by 3.5 kg in S2 and was increased by 4.0 kg in S3 after rosiglitazone treatment for 6 months, indicating that rosiglitazone induced adipocyte differentiation in both cases. Adiponectin level was low before treatment and showed slight increase in both cases. Owen et al [23] also reported no clear advantages in treating patients with FPLD caused by a mutation in the *LMNA* gene (R482W) with rosiglitazone despite increases in subcutaneous adipose tissue. The effects of TZDs on glycemic control, body weight, and adiponectin thus appear to vary in patients with various forms of FPLD [14,18,22-24].

We also measured changes in fat and lean mass during pioglitazone treatment by DEXA scan. As shown in Table 4, fat mass increased by 2.2kg, whereas lean mass increased by 0.7 kg during pioglitazone treatment. Table 4 also shows that subcutaneous fat in the abdomen increased during pioglitazone treatment, consistent with a previous report [7]. Pioglitazone induced increase in fat mass almost equally in the upper limbs, lower limbs, and trunk, although the increase was less in the lower limbs than in the other 2 regions, suggesting a defect in adipocyte differentiation in the lower limbs where fat atrophy exists. Pioglitazone may thus improve glycemic control through adipocyte differentiation from progenitor cells mainly in the upper limbs and trunk [25,26].

Garg [27] has reported that women with Dunnigan-type FPLD have twice the prevalence of diabetes and more than 3 times the prevalence of atherosclerotic vascular disease as men. The mother of our patient with partial lipodystrophy had diabetes and died of cerebral infarction. Regular evaluation for atherosclerosis will therefore be required in this patient.

In conclusion, we have described the phenotype of a case of FPLD case of Asian origin, which differs from that of FPLD cases of European origin. As there were no mutations in the causative genes of *LMNA*, *PPARG*, *AKT2*, caveolin-1, and *PPARG4* promoter, known to be associated with FPLD, it may be that a novel gene is involved in this case. More FPLD cases of Asian origin will need to be examined to determine the clinical features, phenotype, and genotype of Asian cases of FPLD.

Acknowledgment

We thank Dr Takashi Shiokawa (Tanita, Tokyo, Japan) for providing us with the DEXA data of 55 healthy women between the ages of 40 and 49 years.

References

[1] Garg A. Acquired and inherited lipodystrophies. N Eng J Med 2004;350:1220-34.
[2] Agarwal AK, Garg A. Genetic disorders of adipose tissue development, differentiation and death. Annu Rev Genomics Hum Genet 2006;7:175-99.
[3] Agarwal AK, Garg A. Genetic basis of lipodystrophies and management of metabolic complications. Annu Rev Med 2006;57:297-311.
[4] Ebihara K, Kusakabe T, Hirata M, Masuzaki H, Miyanaga F, Kobayashi N, et al. Efficacy and safety of leptin-replacement therapy and possible mechanisms of leptin actions in patients with generalized lipodystrophy. J Clin Endocrinol Metab 2007;92:532-41.
[5] Dunnigan MG, Cochrane MA, Kelly A, Scott JW. Familial lipoatrophic diabetes with Dominant transmission. Q J Med 1974; 169:33-48.
[6] Arita Y, Kihara S, Ouchi Nm Takahashi M, Maeda K, Miyagawa J, Hotta K, et al. Paradoxical decrease of an adipose-specific protein, adiponectin, in obesity. Biochem Biophys Res Commun 1999;257: 79-83.
[7] Akazawa S, Kawasaki E, Sun F, Eguchi K, Ito M. Efficacy of troglitazone on body fat distribution type 2 diabetes. Diabetes Care 2000;23:1067-71.
[8] Sandre-Giovannoli AD, Chaouch M, Kozlov S, Vallat JM, Tazir M, Kassouri N, et al. Homozygous defects in *LMNA*, encoding lamin A/C nuclear-envelope proteins, cause autosomal recessive axonal neuropathy

in human (Charcot-Marie-Tooth disorder type 2) and mouse. Am J Hum Genet 2002;70:726-36.

[9] Elbrecht A, Chen Y, Cullinan CA, Hayers N, Leibowitz MD, Moller DE, et al. Molecular cloning, expression and characterization of Human peroxisome proliferator activated receptors r1 and r2. Biochem Biophys Res Commun 1996;224:431-7.

[10] George S, Rochford JJ, Wolfrum C, Gray SL, Schinner S, Wilson JC, et al. Family with severe insulin resistance and diabetes due to a mutation in *AKT2*. Science 2004;304:1325-8.

[11] Kim CA, Delepine M, Boutet E, Mourabit HE, Lay SL, Meier M, et al. Association of a homozygous nonsense caveolin-1 mutation with Berardinelli-Seip congenital lipodystrophy. J Clin Endocrinol Metab 2008;93:1129-34.

[12] Shali KA, Cao H, Knoers N, Hermus R, Tack CJ, Hegele RA. A single-base mutation in the peroxisome proliferator–activated receptor G4 promotor associated with altered in vitro expression and partial lipodystrophy. J Clin Endocrinol Metab 2004;89:5655-60.

[13] Johansen K, Rasmussen MH, KJEMS LL, Astrup A. An unusual type of familial lipodystrophy. J Clin Endocrinol Metab 1995;80:1106-18.

[14] Sleilati GG, Leff T, Bonnett JW, Hegele R. Efficacy and safety of pioglitazone in treatment of a patient with an atypical lipodystrophy syndrome. Endocri Pract 2007;13:656-61.

[15] Cao H, Alston L, Rushman J, Hegele RA. Heterozygous CAVI frameshift mutation (MIM601047) in patients with atypical partial lipodystrophy and hypertriglyceridemia. Lipids in Heath and Disease 2008;7:3.

[16] Garg A, Agawal AK. Caveolin-1: a new locus for human lipodystrophy. J Clin Endocrinol Metab 2008;93(4):1183-5.

[17] Shackleton S, Lloyd DJ, Jackson SNJm Evans R, Niermeijer MF, Singh BM, Schmidt H, et al. *LMNA*, encoding lamin A/C, is mutated in partial lipodystrophy. Nat Genet 2000;24:153-6.

[18] Savage DB, Tan GD, Acerini CL, Jebb SA, Agostini M, Gurnell M, et al. Human metabolic syndrome resulting from dominant-negative mutations in the nuclear receptor peroxisome proliferator–activated receptor–G. Diabetes 2003;52:910-7.

[19] Hegele RA, Cao H, Frankowski C, Mathews S, Leff T. *PPARG* F388L, a transactivation-deficient mutant, in familial partial lipodystrophy. Diabetes 2002;51:3586-90.

[20] Agarwal AK, Grag AA. Novel heterozygous mutation in peroxisome proliferator–activated receptor–G gene in a patient with familial partial lipodystrophy. J Clin Endocrinol Metab 2002;87:408-11.

[21] Kadowaki T, Kadowaki H, Taylor SI. A nonsense mutation causing decreased levels of insulin receptor mRNA: detection by a simplified technique for direct sequencing of genomic DNA amplified by the polymerase chain reaction. ProcNatlAcadSciUSA 1990;87:658-62.

[22] Arioglu EA, Duncan-Morin J, Sebring N, Rother KI, Gottlieb N, Hoofnagle AE, et al. Efficacy and safety of troglitazone in the treatment of lipodystrophy syndromes. Ann Intern Med 2000;133: 263-74.

[23] Owen KR, Donohoe M, Ellard S, Hattersley AT. Response to treatment with rosiglitazone in familial partial lipodystrophy due to a mutation in the *LMNA* gene. Diabet Med 2003;20:823-7.

[24] Ludtke A, Heckt K, Geneschel J, Mehnert H, Spuler S, Worman J, et al. Long-term treatment experience in a subject with Dunnigan-type familial partial lipodystrophy: efficacy of rosiglitazone. Diabet Med 2005;22:1611-3.

[25] Lewis GF, Carpentier A, Adeli K, Glacca A. Disordered fat storage and mobilization in the pathogenesis of insulin resistance and type 2 diabetes. Endocrine Reviews 2002;23:201-29.

[26] Smith SA. Central role of the adipocyte in the insulin-sensitising and cardiovascular risk modifying action of the thiazolidinediones. Biochime 2003;85:1219-30.

[27] Garg A. Gender differences in the prevalence of metabolic complications in familial partial lipodystrophy (Dunnigan variety). J Clin Endocrinol Metab 2000;85:1776-82.

Generation of Transgenic Mice Overexpressing a Ghrelin Analog

Go Yamada, Hiroyuki Ariyasu, Hiroshi Iwakura, Hiroshi Hosoda, Takashi Akamizu, Kazuwa Nakao, and Kenji Kangawa

Department of Endocrinology and Metabolism (G.Y., K.N.), Kyoto University Graduate School of Medicine, and Ghrelin Research Project (H.A., H.I., T.A., K.K.), Translational Research Center, Kyoto University Hospital, Kyoto 606-8507, Japan; and Department of Biochemistry (H.H., K.K.), National Cardiovascular Center Research Institute, Osaka 565-8565, Japan

After the discovery of ghrelin, we attempted to generate ghrelin gene transgenic (Tg) mice. These animals, however, produced only des-acyl ghrelin, which lacked the n-octanoyl modification at Ser^3 necessary to manifest ghrelin activity. Because the mechanism for acyl-modification of ghrelin had been unclear until the recent identification of GOAT (ghrelin O-acyltransferase), it had been difficult to generate Tg mice overexpressing ghrelin using standard procedures. Therefore, we planned to generate Tg mice overexpressing a ghrelin analog, which possessed ghrelin-like activity in the absence of acylation at Ser^3 and could be synthesized *in vivo*. As the replacement of Ser^3 of ghrelin with Trp^3 (Trp^3-ghrelin) preserves a low level of ghrelin activity and Trp^3-ghrelin can be synthesized *in vivo*, we generated mice overexpressing Trp^3-ghrelin by using the hSAP (human serum-amyloid-P) promoter. Plasma Trp^3-ghrelin concentrations in the Tg mice were approximately 85-fold higher than plasma ghrelin concentrations in non-Tg littermates. Because Trp^3-ghrelin is approximately 1/10–1/20 less potent than ghrelin *in vivo*, plasma Trp^3-ghrelin concentrations in Tg mice were calculated to have an activity approximately 6-fold greater than that of acylated ghrelin seen in non-Tg mice (85-fold x 1/10–1/20). Tg mice exhibited a normal growth and glucose metabolism in their early life stage. However, 1-yr-old Tg mice demonstrated impaired glucose tolerance and reduced insulin sensitivity. This model will be useful to evaluate the long-term effects of ghrelin or ghrelin analogs. In addition, this technique may be a useful method to generate gain-of-activity models for hormones that require posttranscriptional modifications. (***Endocrinology* 151: 5935–5940, 2010**)

Ghrelin, an endogenous ligand for the GH secretagogue receptor (GHS-R) (or ghrelin receptor), is a stomach-derived 28-amino acid peptide hormone modified by n-ontanoylic acid at the third Ser residue (Ser^3) (1). This modification is essential for ghrelin activity (1).

Since ghrelin was discovered, several groups, including us, have been trying to generate transgenic (Tg) mice overexpressing ghrelin under the control of different promoters (2–7). All of these animals, with the exception of two lines created by Reed *et al.* (5) and Bewick *et al.* (8), produced des-acyl ghrelin only. This form lacks the n-octanoyl modification at Ser^3 and is devoid of ghrelin activity. The mechanism for ghrelin acylation had been unclear until the recent identification of ghrelin O-acyltransferase (GOAT) (9). Because GOAT had not yet been identified when we initiated this study and it had proved to be difficult to generate the Tg mice overexpressing ghrelin by standard procedures, we planned to generate Tg mice overexpressing a ghrelin analog possessing ghrelin-like activity without Ser^3 acylation that could be synthesized *in vivo*.

Matsumoto *et al.* (10) investigated the effect on ghrelin bioactivities of replacement of the octanoylated Ser at the third position with other amino acids, such as tryptophan

ISSN Print 0013-7227 ISSN Online 1945-7170
Printed in U.S.A.

doi: 10.1210/en.2010-0635 Received June 4, 2010. Accepted September 20, 2010.
First Published Online October 20, 2010

Abbreviations: C-RIA, RIA recognizing the C-terminal region of ghrelin; GOAT, ghrelin O-acyltransferase; GHS-R, GH secretagogue receptor; hSAP, human serum-amyloid-P; N-RIA, RIA recognizing the N-terminal region of ghrelin; Tg, transgenic; Trp, tryptophan; Trp^3-ghrelin, ghrelin analog with the third amino-acid residue (Ser^3) replaced by Trp.

(Trp), Val, Leu, or Ile. The ghrelin-like activity of these synthetic peptides was evaluated by EC_{50} values, determined by an increase in intracellular calcium concentrations $[Ca^{2+}]_i$ in GHS-R-expressing cells. Replacement of Ser^3 with Trp^3 (Trp^3-ghrelin) preserved ghrelin activity with an EC_{50} of 31 nM in comparison with 1.3 nM for intact ghrelin. Replacement of Ser^3 with Val^3, Leu^3, or Ile^3 led to complete loss of ghrelin potency. Although ghrelin analog, in which the Ser^3 residue was replaced by Trp (Trp^3-ghrelin) is approximately 24-fold less active than native ghrelin *in vitro*, it can be synthesized *in vivo*. Thus, we selected Trp^3-ghrelin as a candidate ghrelin analog.

In this study, we examined whether Trp^3-ghrelin exerts ghrelin-like activity *in vivo*. After confirming this activity, we generated Tg mice overexpressing Trp^3-ghrelin.

Materials and Methods

All animal protocols were approved by the Kyoto University Graduate School of Medicine Committee on Animal Research. Animals, housed in air-conditioned animal quarters with light between 0800 and 2000 h, were maintained on standard rat chow (CE-2, 352 kcal/100 g; Japan CLEA, Osaka, Japan).

Experiment 1, the *in vivo* effects of Trp^3-ghrelin

Eight-week-old male C57BL/6 mice were purchased from Japan CLEA. Ghrelin was obtained from Peptide Research Institute (Osaka, Japan). Trp^3-ghrelin, in which the Ser^3 residue was replaced by Trp, was synthesized as previously described (10).

Food intake

Mice (n = 8, each group) were injected sc with saline, ghrelin (120 or 360 mcg/kg), or Trp^3-ghrelin (360, 1200, or 3600 mcg/kg) before measuring a 2-h food intake.

GH secretion

Mice (n = 8, each group) were injected with iv saline, ghrelin (4, 12, 40, or 120 mcg/kg), or Trp^3-ghrelin (12, 40, 120, or 360 mcg/kg). Blood samples were collected from the retro-orbital vein 10 min after injection and stored at −20 C until assessed.

Inhibition of glucose stimulated insulin secretion

After a 12-h fast, mice (n = 8, each group) were injected iv with 1.0 g/kg glucose, together with saline, ghrelin (120 or 360 mcg/kg), or Trp^3-ghrelin (1200 or 3600 mcg/kg). Blood samples were collected 1 and 10 min after injection and stored at −20 C until assessed.

Experiment 2, generation of Tg mice overexpressing a ghrelin analog, Trp^3-ghrelin

Plasmid construction and generation of Tg mice

We generated a fusion gene of the human serum-amyloid-P (hSAP) promoter and full-length mouse preproghrelin cDNA (1, 11). Plasmid hSAP-ghrelin was constructed by inserting mouse preproghrelin cDNA into the unique *Eco*RI site between the hSAP promoter and the 3′-flanking sequence of the rabbit β-globin gene. Mutations were created using a QuikChange Site-Directed Mutagenesis kit, according to the manufacturer's instruction. The hSAP-ghrelin plasmid was used as the template for PCR amplification. To replace the AGC codon encoding Ser to a TGG codon encoding Trp, we used two oligonucleotide primers: 5′-GGACATGGCCATGGCAGGCTCCTGGTTCCTGAGCCCAGAGC-3′ and 5′-GCTCTGGGCTCAGGAACCAGGAGCCTGCCATGGCCATGTCC-3′. The mutated construct was verified by sequencing (please see figure 2A). The DNA fragment encoding mutant ghrelin was excised from the plasmid by digestion with *Sal*I and *Hin*dIII (see figure 2B), then purified and microinjected into the pronuclei of fertilized eggs as reported (11). Founder Tg mice were identified by PCR analysis and bred against C57BL/6 mice.

Please refer to Supplemental Methods, published on The Endocrine Society's Journals Online web site at http://endo.endojournals.org, for real-time quantitative RT-PCR, semiquantitative PCR, glucose and insulin tolerance tests, measurements of insulin-releasing ability, body weights, body length, body composition, daily food intake, hormonal parameters, and statistical analyses.

Results

Experiment 1, the *in vivo* effects of Trp^3-ghrelin on food intake and GH secretion

To elucidate whether Trp^3-ghrelin has ghrelin-like potency *in vivo*, 8-wk-old male C57BL/6 mice were administrated vehicle, ghrelin, or Trp^3-ghrelin before determining food intake over a period of 2 h. Injection of ghrelin or Trp^3-ghrelin stimulated food intake in a dose-dependent manner (Fig. 1A). The 2-h food intake after injection of 3600 mcg/kg of Trp^3-ghrelin was 0.47 ± 0.04 g, which was 2.2-fold higher than that seen in vehicle-injected mice (0.21 ± 0.02 g/2 h). This level of stimulation was similar to that seen in mice injected with ghrelin at a dose of 360 mcg/kg. Serum GH levels increased after injection of 360 mcg/kg Trp^3-ghrelin to 133.9 ± 46.1 ng/ml, which was 21-fold higher than that seen after vehicle injection (6.4 ± 1.1 ng/ml) and similar to those seen after ghrelin injection at 40 mcg/kg (138.8 ± 26.5 ng/ml, respectively) (Fig. 1B). Injection of ghrelin or Trp^3-ghrelin inhibited glucose-stimulated insuline release in a dose-dependent manner (Fig. 1C). The 10-min insulin response was significantly inhibited by 3600 mcg/kg Trp^3-ghrelin and 360 mcg/kg to the same extent (0.78 ± 0.09 and 0.63 ± 0.06 ng/ml), compared with saline (1.10 ± 0.01 ng/ml). These results indicated that Trp^3-ghrelin stimulates food intake and GH secretion and inhibits glucose-stimulated insulin secretion in a manner similar to ghrelin with a potency approximately 1/10–1/20 (Trp^3-ghrelin needs about 20-fold amount for stimulation of food intake, about 10-fold amount for GH secretion, and about 10-fold amount for

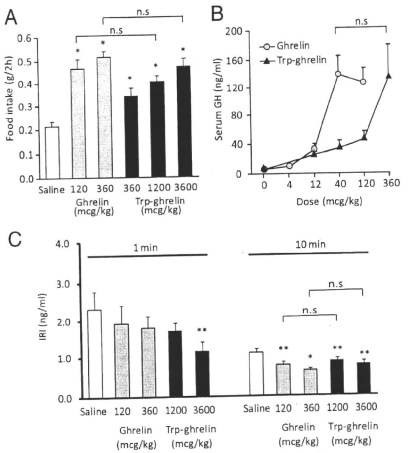

FIG. 1. Effects of the exogenous administration of Trp^3-ghrelin on food intake, GH secretion, and inhibition of glucose stimulated insulin release. A, Two-hour food intake after saline (*open bar*), ghrelin at 120 or 360 mcg/kg (*shaded bars*), or Trp^3-ghrelin at 360, 1200, or 3600 mcg/kg (*closed bars*) ip injection (n = 8–10). B, Serum GH levels were measured 10 min after 4, 12, 40, or 120 mcg/kg ghrelin (*shaded circles*) or 12, 40, 120, or 360 mcg/kg Trp^3-ghrelin (*closed triangles*) iv injection (n = 8–10). C, Serum insulin levels were measured 1 and 10 min after iv injection of 1.0 g/kg glucose, together with saline (*open bars*), ghrlein (120 and 360 mcg) (*shaded bars*), or Trp^3-ghrelin (1200 and 3600 mcg/kg) (*closed bars*) (n = 8). *, $P < 0.01$; **, $P < 0.05$; n.s, not significant compared with saline group; IRI, immunoreactive insulin. Data are presented as the means ± SEM.

inhibition of glucose stimulated insulin release) that of ghrelin.

Experiment 2, generation of Tg mice overexpressing Trp^3-ghrelin

Two Tg mouse lines, Tg6-2 and Tg6-5, were obtained. Hepatic transgene expression in Tg6-2 and Tg6-5 mice was 3.02 ± 1.15 and 0.07 ± 0.01 in arbitrary units, respectively, after normalization to preproghrelin mRNA expression levels seen in the stomachs of non-Tg littermates (non-Tg mice) (1.00 ± 0.18). No expression of preproghrelin mRNA was seen in the livers of non-Tg mice (Fig. 2C).

Two RIA methods [RIA recognizing the N-terminal region of ghrelin (N-RIA) and RIA recognizing the C-terminal region of ghrelin (C-RIA)] were performed to measure plasma ghrelin, des-acyl ghrelin, and Trp^3-ghrelin concentrations. In a previous study, N-RIA has been demonstrated to recognize only the acylated N-terminal region of ghrelin, whereas C-RIA recognizes the C-terminal region of ghrelin, making it possible to detect both acylated ghrelin and des-acyl ghrelin (12). We determined whether Trp^3-ghrelin could be detected by one or both of these RIA systems. When synthetic Trp^3-ghrelin was added to plasma samples from wild-type mice, Trp^3-ghrelin could only be detected by C-RIA, not N-RIA (data not shown). At 8 wk of age, plasma ghrelin concentrations measured by N-RIA did not differ among genotypes. Total plasma ghrelin concentrations, including ghrelin, des-acyl ghrelin, and Trp^3-ghrelin, measured by C-RIA were significantly elevated in Tg mice (Fig. 2, D and E). To determine precise plasma Trp^3-ghrelin concentration, we also performed HPLC on Tg6-2 samples (Fig. 2F). Plasma ghrelin (40.5 ± 10.2 *vs.* 36.6 ± 4.4 fmol/ml) and des-acyl ghrelin (167.5 ± 51.8 *vs.* 235.7 ± 44.8 fmol/ml) concentrations did not differ among genotypes.

Plasma Trp^3-ghrelin concentrations in Tg6-2 was 3437.8 ± 571.6 (2546.4–5101.7) fmol/ml, which was approximately 85-fold (3437.8/40.5 = 84.9-fold) higher than plasma ghrelin (acylated ghrelin) concentrations seen in non-Tg mice. Because Trp^3-ghrelin is approximately 1/10–1/20 less potent than ghrelin *in vivo* (experiment 1), plasma Trp^3-ghrelin concentrations in Tg6-2 were calculated to have an activity approximately 6-fold greater than that of ghrelin (acylated ghrelin) seen in non-Tg mice (84.9-fold × 1/10–1/20 = 4.2–8.5-fold). Total ghrelin concentrations measured by C-RIA in the Tg mice were roughly constant throughout the day.

We then analyzed the phenotype of the Tg6-2 line. Tg mice overexpressing Trp^3-ghrelin (Tg6-2 line) were abbreviated as Trp^3-ghrelin-Tg mice.

The analysis of the phenotypes of Trp^3-ghrelin-Tg mice

During postnatal development, there were no significant differences in somatic growth between Trp^3-ghrelin-Tg and non-Tg mice (Supplemental Fig. 1, A and B). Consistent with these results, no changes in serum GH and IGF-I concentrations were observed in Trp^3-ghrelin-Tg mice (Supplemental Fig. 1, C and D). The average food intake of Trp^3-ghrelin-Tg mice did not differ from that of non-Tg mice (Supplemental Fig. 1E). Trp^3-ghrelin-Tg mice consumed the largest food portions during the dark phase (75.4 ± 2.7%), similar to the behavior seen in non-Tg mice (75.9 ± 1.6%). There were no differences between 10-wk-old Trp^3-ghrelin-Tg and non-Tg mice in pituitary and hypothalamic mRNA levels of factors involved in GH secretion and food intake (Supplemental Fig. 2, A and B). In addition, glucose metabolism in Trp^3-ghrelin-Tg mice did not differ from that seen in non-Tg mice in early life (Supplemental Fig. 1, F and G).

We conducted a precise evaluation of glucose metabolism using more aged mice. Thus we continued rearing

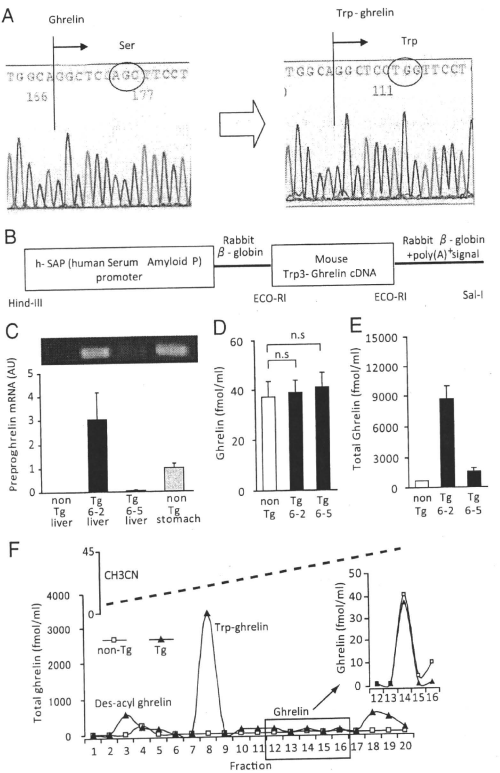

FIG. 2. Generation of Trp^3-ghrelin overexpressing Tg mice. A, A mutant construct in which the AGC codon encoding Ser, the third amino acid of ghrelin that is modified by n-octanoic acid, was replaced by a TGG codon encoding Trp. B, The construct encoding Trp^3-ghrelin used to generate Tg mice was a fusion gene of the hSAP promoter combined with the mutated cDNA of mouse ghrelin. C, The expression levels of preproghrelin mRNA or mutated preproghrelin mRNA. D, Plasma concentrations of ghrelin (acylated form) were measured by N-RIA (n = 8–10). E, Plasma concentrations of total ghrelin, which included ghrelin, des-acyl ghrelin, and Trp^3-ghrelin, were measured by C-RIA (n = 8–10). F, Representative results of HPLC analysis (non-Tg, *open square*; Tg6-2, *closed triangle*). n.s, Not significant. Data are presented as the means ± SEM (C–E).

these mice to 1 yr of age. Some intriguing results on glucose metabolism were obtained from 1-yr-old Trp^3-ghrelin-Tg mice. Although there were no differences between Trp^3-ghrelin-Tg and non-Tg mice in anthropometric parameters, including body weight, total body fat percentage, and lean body mass, Trp^3-ghrelin-Tg mice exhibited impaired glucose tolerance and reduced insulin sensitivity (Fig. 3, A–F); blood glucose levels after glucose injection were significantly higher than those in non-Tg mice. The acute phase of insulin secretion typically seen in response to glucose tended to be suppressed in Trp^3-ghrelin-Tg mice (P = 0.11) (Fig. 3, C and D). In addition, the hypoglycemic response after the injection with insulin was blunted in Trp^3-ghrelin-Tg mice (Fig. 3E). There were no differences, however, in pancreatic insulin mRNA levels between 1-yr-old Trp^3-ghrelin-Tg and non-Tg mice (Fig. 3F). Because glucose tolerance and insulin sensitivity are influenced by GH, we examined whether GH secretion was augmented in 1-yr-old Trp^3-ghrelin-Tg mice. Serum GH and IGF-I levels were unchanged in Trp^3-ghrelin-Tg mice in comparison with those seen in non-Tg mice at 1 yr of age (Fig. 4, A and B). There was no difference between 1-yr-old Trp^3-ghrelin-Tg and non-Tg mice in ghrelin or GOAT mRNA within the stomach or in plasma acylated ghrelin concentrations, which reflects the intrinsic secretion of ghrelin (Fig. 4, C and D). Because ghrelin can also affect the lipid metabolism, we measured serum nonesterified fatty acid, total cholesterol, and triglyceride levels. However, there was no significant difference in them (non-Tg *vs.* Tg: nonesterified fatty acid, 0.74 ± 0.03 *vs.* 0.82 ± 0.04 mEq/liter, P = 0.12; total cholesterol, 122.5 ± 9.8 *vs.* 143.4 ± 7.4 mg/dl, P = 0.10; triglyceride, 162.6 ± 12.8 *vs.* 159.5 ± 10.8 mg/dl, P = 0.85).

Discussion

It is challenging to generate ghrelin gain-of-activity models, because ghrelin requires posttranscriptional modification, an octanoylation of Ser^3. GOAT is responsible for this octanoylation of ghrelin, which confers its biological activity (10, 13). In this study, we succeeded in generating Tg mice overexpressing Trp^3-ghrelin, a ghrelin analog that does not require posttranscriptional modification with GOAT for activity. Because expression of the mutated-ghrelin transgene was driven by the hSAP promoter, Trp^3-ghrelin was continuously secreted from the liver after birth. Plasma concentrations of Trp^3-ghrelin of Tg mice were calculated to have an equivalent activity

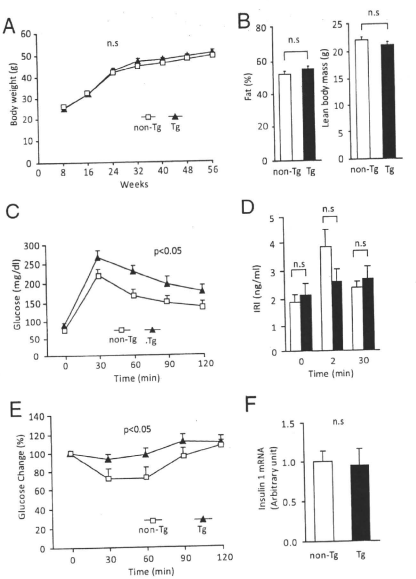

FIG. 3. Analysis of Trp^3-ghrelin Tg mice. A, Changes of body weight in Trp^3-ghrelin-Tg mice (*closed triangles*) and non-Tg littermates (*open squares*) (n = 20–25). B, Body fat percentage and lean body mass, as determined by computer tomography, in 52-wk-old Trp^3-ghrelin-Tg mice (*closed bars*) and non-Tg littermates (*open bars*) (n = 14–16). C, Glucose tolerance test (0.75 g/kg) was performed in 52-wk-old Trp^3-ghrelin-Tg mice (*closed triangles*) and non-Tg littermates (*open squares*) (n = 14–16; *, $P < 0.05$ in comparison with non-Tg littermates). D, Serum insulin levels at baseline, 2 min, and 30 min after ip glucose injection of 52-wk-old Trp^3-ghrelin-Tg mice (*closed bars*) and non-Tg littermates (*open bars*) (n = 14–16, $P = 0.11$ in comparison with non-Tg littermates). E, Insulin tolerance test after treatment with 1.5 U/kg regular insulin in 52-wk-old Trp^3-ghrelin-Tg mice (*closed triangles*) and non-Tg littermates (*open squares*) (n = 14–16; *, $P < 0.05$ in comparison with non-Tg littermates). F, Insulin 1 mRNA levels in the pancreases of 52-wk-old Trp^3-ghrelin-Tg mice (*closed bars*) and non-Tg littermates (*open bars*) (n = 14). IRI, Immunoreactive insulin; n.s, not significant. Data are presented as the means ± SEM.

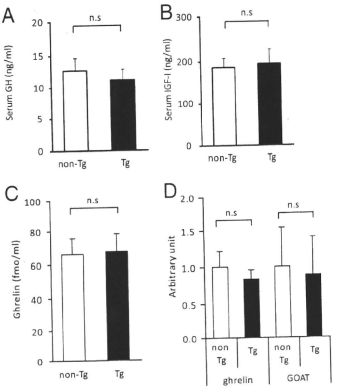

FIG. 4. We examined the levels of GH/IGF-I axis factors, plasma ghrelin levels, and ghrelin and GOAT mRNA levels in the stomachs of 52-wk-old Trp^3-ghrelin-Tg mice. A and B, We measured serum GH (A) and IGF-I (B) levels in 52-wk-old Trp^3-ghrelin-Tg mice (*closed bars*) and non-Tg littermates (*open bars*) (n = 10). C, Plasma ghrelin levels in 52-wk-old Trp^3-ghrelin-Tg mice (*closed bars*) and non-Tg littermates (*open bars*) (n = 10). D, The mRNA levels of ghrelin and GOAT in the stomachs of 52-wk-old Trp^3-ghrelin-Tg mice (*closed bars*) and non-Tg littermates (*open bars*) (n = 14). n.s, Not significant. Data are presented as the means ± SEM.

as 4.2- to 8.5-fold higher levels of acylated ghrelin in non-Tg mice. We think that this unique mouse model is a useful tool to evaluate the long-term pathophysiological and/or pharmacological effects of ghrelin or ghrelin analogs and provides insight into the physiological roles of ghrelin/GHS-R systems.

Bewick *et al.* (8) developed ghrelin-overexpressing mice using the endogenous ghrelin promoter. Although this mouse model was suitable to investigate the physiological role of ghrelin, it is not suitable to explore the pathophysiological or pharmacological effects of ghrelin, because the plasma ghrelin levels achieved in these mice were only 1.5-fold greater than that seen in non-Tg mice at the highest. Reed *et al.* (5) also developed ghrelin-overexpressing mice using the neuron-specific enolase promoter, reaching circulating ghrelin levels approximately 5-fold higher than those seen in non-Tg mice. Because these mice primarily produced ghrelin in the brain, it remains unclear whether the phenotype of these mice resulted from elevations in peripheral ghrelin and/or central ghrelin. Kirchner *et al.* (13) generated Tg mice simultaneously expressing human ghrelin and GOAT in the liver under the control of the human apolipoprotein E promoter. When fed a standard diet, these mice lack the circulating fatty-acid-modified forms of ghrelin, demonstrating high circulating concentrations of des-acyl ghrelin only. These mice exhibited elevated concentrations of fatty-acid-modified forms of ghrelin only when given a diet rich in medium-chain triglycerides. It may be difficult to characterize the phenotype of the mice precisely, especially the metabolic phenotype, under such a diet.

Trp^3-ghrelin-Tg mice exhibited normal growth patterns and feeding behaviors. These results are consistent with previous results; ghrelin loss-of-function mice, ghrelin-deficient mice, or ghrelin-receptor-null mice all have normal growth rates, food intake, and body compositions (14–17). One-year-old Trp^3-ghrelin-Tg mice demon-

strated impaired glucose tolerance and reduced insulin sensitivity, although there were no differences in body weight or composition between Trp^3-ghrelin-Tg and non-Tg mice. When ghrelin-receptor-null mice were maintained on long-term standard chow, they had lower blood glucose levels with low-to-normal insulin levels in comparison with wild-type mice, although they exhibited similar body weights and composition (14). Ghrelin-receptor-null mice appeared to have enhanced insulin sensitivity in comparison with wild-type mice. In addition, Gauna *et al.* (18) demonstrated that administration of ghrelin to wild-type mice reduced insulin sensitivity. It was also reported that ghrelin inhibited glucose-stimulated insulin release (19–21).

In conclusion, we succeeded in generating Tg mice overexpressing a ghrelin analog. The mice presented in this study will serve as a useful tool for evaluating the long-term effects of ghrelin or ghrelin analogs. In addition, the method provided in this study may be useful in the generation of gain-of-function models for hormones that require posttranscriptional modification.

Acknowledgment

Address all correspondence and requests for reprints to: Hiroyuki Ariyasu, M.D., Ph.D., Ghrelin Research Project, Translational Research Center, Kyoto University Hospital, 54 Shogin Kawahara-cho, Sakyo-ku, Kyoto 606-8507, Japan. E-mail: ariyasu@kuhp.kyoto-u.ac.jp.

This work was supported by grants from the Ministry of Education, Culture, Sports, Science, and Technology of Japan and from the Ministry of Health, Labor, and Welfare of Japan; and by research grants from the Program for the Promotion of Fundamental Studies in Health Sciences of the National Institute of Biomedical Innovation.

Disclosure Summary: The authors have nothing to disclose.

References

1. **Kojima M, Hosoda H, Date Y, Nakazato M, Matsuo H, Kangawa K** 1999 Ghrelin is a growth-hormone-releasing acylated peptide from stomach. Nature 402:656–660
2. **Ariyasu H, Takaya K, Iwakura H, Hosoda H, Akamizu T, Arai Y, Kangawa K, Nakao K** 2005 Transgenic mice overexpressing desacyl ghrelin show small phenotype. Endocrinology 146:355–364
3. **Asakawa A, Inui A, Fujimiya M, Sakamaki R, Shinfuku N, Ueta Y, Meguid MM, Kasuga M** 2005 Stomach regulates energy balance via acylated ghrelin and desacyl ghrelin. Gut 54:18–24
4. **Iwakura H, Hosoda K, Son C, Fujikura J, Tomita T, Noguchi M, Ariyasu H, Takaya K, Masuzaki H, Ogawa Y, Hayashi T, Inoue G, Akamizu T, Hosoda H, Kojima M, Itoh H, Toyokuni S, Kangawa K, Nakao K** 2005 Analysis of rat insulin II promoter-ghrelin transgenic mice and rat glucagon promoter-ghrelin transgenic mice. J Biol Chem 280:15247–15256
5. **Reed JA, Benoit SC, Pfluger PT, Tschöp MH, D'Alessio DA, Seeley RJ** 2008 Mice with chronically increased circulating ghrelin develop age-related glucose intolerance. Am J Physiol Endocrinol Metab 294:E752–E760
6. **Wei W, Qi X, Reed J, Ceci J, Wang HQ, Wang G, Englander EW, Greeley Jr GH** 2006 Effect of chronic hyperghrelinemia on ingestive action of ghrelin. Am J Physiol Regul Integr Comp Physiol 290: R803–R808
7. **Zhang W, Chai B, Li JY, Wang H, Mulholland MW** 2008 Effect of des-acyl ghrelin on adiposity and glucose metabolism. Endocrinology 149:4710–4716
8. **Bewick GA, Kent A, Campbell D, Patterson M, Ghatei MA, Bloom SR, Gardiner JV** 2009 Mice with hyperghrelinemia are hyperphagic and glucose intolerant and have reduced leptin sensitivity. Diabetes 58:840–846
9. **Yang J, Brown MS, Liang G, Grishin NV, Goldstein JL** 2008 Identification of the acyltransferase that octanoylates ghrelin, an appetite-stimulating peptide hormone. Cell 132:387–396
10. **Matsumoto M, Kitajima Y, Iwanami T, Hayashi Y, Tanaka S, Minamitake Y, Hosoda H, Kojima M, Matsuo H, Kangawa K** 2001 Structural similarity of ghrelin derivatives to peptidyl growth hormone secretagogues. Biochem Biophys Res Commun 284:655–659
11. **Ogawa Y, Masuzaki H, Hosoda K, Aizawa-Abe M, Suga J, Suda M, Ebihara K, Iwai H, Matsuoka N, Satoh N, Odaka H, Kasuga H, Fujisawa Y, Inoue G, Nishimura H, Yoshimasa Y, Nakao K** 1999 Increased glucose metabolism and insulin sensitivity in transgenic skinny mice overexpressing leptin. Diabetes 48:1822–1829
12. **Ariyasu H, Takaya K, Hosoda H, Iwakura H, Ebihara K, Mori K, Ogawa Y, Hosoda K, Akamizu T, Kojima M, Kangawa K, Nakao K** 2002 Delayed short-term secretory regulation of ghrelin in obese animals: evidenced by a specific RIA for the active form of ghrelin. Endocrinology 143:3341–3350
13. **Kirchner H, Gutierrez JA, Solenberg PJ, Pfluger PT, Czyzyk TA, Willency JA, Schürmann A, Joost HG, Jandacek RJ, Hale JE, Heiman ML, Tschöp MH** 2009 GOAT links dietary lipids with the endocrine control of energy balance. Nat Med 15:741–745
14. **Zigman JM, Nakano Y, Coppari R, Balthasar N, Marcus JN, Lee CE, Jones JE, Deysher AE, Waxman AR, White RD, Williams TD, Lachey JL, Seeley RJ, Lowell BB, Elmquist JK** 2005 Mice lacking ghrelin receptors resist the development of diet-induced obesity. J Clin Invest 115:3564–3572
15. **Sun Y, Ahmed S, Smith RG** 2003 Deletion of ghrelin impairs neither growth nor appetite. Mol Cell Biol 23:7973–7981
16. **Sun Y, Wang P, Zheng H, Smith RG** 2004 Ghrelin stimulation of growth hormone release and appetite is mediated through the growth hormone secretagogue receptor. Proc Natl Acad Sci USA 101:4679–4684
17. **Wortley KE, Anderson KD, Garcia K, Murray JD, Malinova L, Liu R, Moncrieffe M, Thabet K, Cox HJ, Yancopoulos GD, Wiegand SJ, Sleeman MW** 2004 Genetic deletion of ghrelin does not decrease food intake but influences metabolic fuel preference. Proc Natl Acad Sci USA 101:8227–8232
18. **Gauna C, Meyler FM, Janssen JA, Delhanty PJ, Abribat T, van Koetsveld P, Hofland LJ, Broglio F, Ghigo E, van der Lely AJ** 2004 Administration of acylated ghrelin reduces insulin sensitivity, whereas the combination of acylated plus unacylated ghrelin strongly improves insulin sensitivity. J Clin Endocrinol Metab 89: 5035–5042
19. **Reimer MK, Pacini G, Ahrén B** 2003 Dose-dependent inhibition by ghrelin of insulin secretion in the mouse. Endocrinology 144:916–921
20. **Iwakura H, Ariyasu H, Li Y, Kanamoto N, Bando M, Yamada G, Hosoda H, Hosoda K, Shimatsu A, Nakao K, Kangawa K, Akamizu T** 2009 A mouse model of ghrelinoma exhibited activated growth hormone-insulin-like growth factor I axis and glucose intolerance. Am J Physiol Endocrinol Metab 297:E802–E811
21. **Dezaki K, Sone H, Koizumi M, Nakata M, Kakei M, Nagai H, Hosoda H, Kangawa K, Yada T** 2006 Blockade of pancreatic islet-derived ghrelin enhances insulin secretion to prevent high-fat diet-induced glucose intolerance. Diabetes 55:3486–3493

C-Type Natriuretic Peptide as a New Regulator of Food Intake and Energy Expenditure

Megumi Inuzuka, Naohisa Tamura, Nobuko Yamada, Goro Katsuura, Naofumi Oyamada, Daisuke Taura, Takuhiro Sonoyama, Yasutomo Fukunaga, Kousaku Ohinata, Masakatsu Sone, and Kazuwa Nakao

Department of Medicine and Clinical Science (M.I., N.T., N.Y., G.K., N.O., D.T., T.S., Y.F., M.S., K.N.), Kyoto University Graduate School of Medicine, Kyoto 606-8507, Japan; and Division of Food Science and Biotechnology (K.O.), Kyoto University Graduate School of Agriculture, Kyoto 611-0011, Japan

The physiological implication of C-type natriuretic peptide (CNP) including energy metabolism has not been elucidated, because of markedly short stature in CNP-null mice. In the present study we analyzed food intake and energy expenditure of CNP-null mice with chondrocyte-targeted CNP expression (CNP-Tg/*Nppc*$^{-/-}$ mice), in which marked skeletal dysplasia was rescued, to investigate the significance of CNP under minimal influences of skeletal phenotypes. In CNP-Tg/*Nppc*$^{-/-}$ mice, body weight and body fat ratio were reduced by 24% and 32%, respectively, at 20 wk of age, and decreases of blood glucose levels during insulin tolerance tests were 2-fold exaggerated at 17 wk of age, as compared with CNP-Tg/*Nppc*$^{+/+}$ mice. Urinary noradrenalin excretion of CNP-Tg/*Nppc*$^{-/-}$ mice was greater than that of CNP-Tg/*Nppc*$^{+/+}$ mice by 28%. In CNP-Tg/*Nppc*$^{-/-}$ mice, rectal temperature at 1600 h was higher by 1.1 C, and uncoupling protein-1 mRNA expression in the brown adipose tissue was 2-fold increased, which was canceled by propranolol administration, as compared with CNP-Tg/*Nppc*$^{+/+}$ mice. Oxygen consumption was significantly increased in CNP-Tg/*Nppc*$^{-/-}$ mice compared with that in CNP-Tg/*Nppc*$^{+/+}$ mice. Food intake of CNP-Tg/*Nppc*$^{-/-}$ mice upon *ad libitum* feeding and refeeding after 48 h starvation were reduced by 21% and 61%, respectively, as compared with CNP-Tg/*Nppc*$^{+/+}$ mice. This study unveiled a new aspect of CNP as a molecule regulating food intake and energy expenditure. Further analyses on precise mechanisms of CNP actions would lead to the better understanding of the significance of the CNP/guanylyl cyclase-B system in food intake and energy expenditure. (***Endocrinology* 151: 3633–3642, 2010**)

C-type natriuretic peptide (CNP) exerts its biological actions using a single-transmembrane guanylyl cyclase (GC), GC-B, which is also known as the natriuretic peptide receptor (NPR)-B, as a receptor (1, 2). CNP was first isolated from porcine brain and expected to be a neuropeptide (3), but the physiological significance of the CNP/GC-B system has been established in the vascular and skeletal systems (1, 4–8). It was reported that CNP and GC-B are expressed in the central and peripheral nervous systems (1, 7, 9–11). The physiological significance of CNP in the nervous system, however, has not been elucidated well. It has been proven that the hypothalamus is an important center to control food intake and energy expenditure (reviewed in Ref. 12). CNP mRNA was detected in the rat hypothalamus, especially in the arcuate nucleus (ARC) and paraventricular nucleus (13), and GC-B mRNA was reportedly expressed in neurons of the magnocellular and parvocellular paraventricular nuclei, the ARC, and the supraoptic nucleus of the rat hypothalamus (14). It is, therefore, speculated that CNP might par-

ISSN Print 0013-7227 ISSN Online 1945-7170
Printed in U.S.A.

doi: 10.1210/en.2010-0141 Received February 3, 2010. Accepted May 18, 2010.
First Published Online June 16, 2010

Abbreviations: AgRP, Agouti-related protein; ARC, arcuate nucleus; BAT, brown adipose tissue; CART, cocaine- and amphetamine-regulated transcript; CNP, C-type natriuretic peptide; CPT, carnitine palmitoyltransferase; D2, type II iodothyronine deiodinase; FFA, free fatty acid; GC, guanylyl cyclase; GTT, glucose tolerance test; icv, intracerebroventricular; ITT, insulin tolerance test; MCH, melanin concentrating hormone; mtTFA, mitochondrial transcription factor A; NPY, neuropeptide Y; PGC, PPARγ-coactivator; POMC, proopiomelanocortin; PPAR, peroxisome proliferator-activated receptor; SNS, sympathetic nervous system; Tg, transgenic; UCP, uncoupling protein; WAT, white adipose tissues; WT, wild type.

ticipate in the regulation of food intake and energy expenditure.

We have shown that the disruption of CNP or GC-B gene (*Nppc* or *Npr2*, respectively) results in dwarfism and early death due to impaired endochondral ossification (7, 8). Although body weight of $Nppc^{-/-}$ or $Npr2^{-/-}$ mice was less than that of wild-type (WT) littermates (7, 8), it was speculated that major causes of their leanness were brain compression and difficulty to eat due to misalignment of tooth between upper and lower jaws, both of which were caused by deformity in the skull and cervical spine (8). Therefore, we generated $Nppc^{-/-}$ mice with chondrocyte-specific CNP expression by crossing $Nppc^{-/-}$ mice and CNP transgenic (Tg) mice that express CNP under the control of the promoter and enhancer of the mouse pro-α1(II) collagen gene (7) and investigated the physiological significance of CNP in the body weight control and metabolic homeostasis with the influence of skeletal problems being minimized.

Materials and Methods

Animals

Male $Nppc^{+/+}$ and $Nppc^{-/-}$ mice with the C57BL/6 genetic background and the transgene that expresses CNP in chondrocytes under the control of the promoter and enhancer of the mouse pro-α1(II) collagen gene (CNP-Tg/$Nppc^{+/+}$ and CNP-Tg/$Nppc^{-/-}$, respectively) were used in this study (7). Intending to completely rescue the dwarf phenotype of $Nppc^{-/-}$ mice, we used mice homozygous for the CNP transgene in this study. Male WT (Non-Tg/$Nppc^{+/+}$) C57BL/6 mice were purchased from Oriental BioService, Kyoto, Japan. Mice were housed in the specified pathogen-free mouse facility of Kyoto University Graduate School of Medicine with unrestricted access to food (F-2, Funabashi Farms, Japan) and water under a 14-h light, 10-h dark cycle (the light cycle is from 0700 h to 2100 h) at 23 C. The genotype of each mouse was determined by PCR using genomic DNA isolated from a tail tip as template, as described previously (7). Primers used are listed in Supplemental Table 1 (published on The Endocrine Society's Journals Online web site at http://endo.endojournals.org). The PCR conditions were the initial denaturation at 95 C for 2 min, followed by 35 cycles of 95 C for 10 sec, 57 C for 10 sec, and 72 C for 30 sec, and the final extension at 72 C for 10 min. Naso-anal length and body weight were measured weekly from 7 d after birth. The experimental protocol of this study was approved by the Animal Research Committee, Kyoto University.

Body fat accumulation and blood and urinary parameters

At 20 wk of age, mice were anesthetized with the ip injection of 50-mg/kg pentobarbital, and epididymal, perirenal, mesenteric, sc white adipose tissues (WAT), and interscapular brown adipose tissue (BAT) were dissected to measure weight. Blood was collected from cardiac ventricles of mice *ad libitum* fed or overnight (1900 h to 1000 h) fasted at 18–20 wk of age under the anesthesia with the ip injection of 50-mg/kg pentobarbital. Blood glucose and serum free fatty acids (FFA) concentrations were measured by a portable glucose meter Glutest Neo (Sanwa Kagaku Kenkyusho, Nagoya, Japan) and a NEFA C-test (Wako Pure Chemical Industries, Osaka, Japan), respectively. Serum concentrations of insulin, leptin, and free T_4 were measured by an ultrasensitive rat insulin ELISA kit with a mouse insulin standard (Morinaga Institute of Biological Science, Kanagawa, Japan), a mouse Leptin ELISA kit (Millipore, Billerica, MA), and an Enzaplate N-FT4 (Bayer Medical, Tokyo, Japan) (15), respectively. Plasma ghrelin concentrations were estimated using an active ghrelin ELISA kit that recognizes n-octanoylated ghrelin (Mitsubishi Kagaku Iatron, Tokyo, Japan) as described previously (16). Mice were individually placed in metabolic cages (Shinano Manufacturing, Tokyo, Japan), and urine samples were collected for 24 h. Urinary noradrenalin concentrations were measured by HPLC in SRL, Tokyo, Japan. The data divided by urinary creatinine concentrations were used to estimate the whole body sympathetic nervous system (SNS) activity.

Glucose and insulin tolerance tests

The glucose tolerance test (GTT) and the insulin tolerance test (ITT) were performed at 17 wk of age. After 4 h fasting (1000 h to 1400 h), mice were ip injected with glucose (0.5 g/kg body weight) or human regular insulin (0.5 U/kg body weight). Blood was collected from a tail vein before the injection, and 30, 60, 90, and 120 min after the injection.

Blood pressure, heart rate, and core body temperature

Blood pressure and heart rate of male mice were measured by a tail-cuff method with a model MK-2000ST (Muromachi Kikai, Tokyo, Japan) at 1000 h to 1200 h. Mice were acclimated to the measurement by experiencing a series of 10 readings once a day for 2 d, and 10 consecutive readings were averaged for each mouse. Rectal temperature was measured as core body temperature with a digital thermometer 02PT (Shibaura Electronics, Saitama, Japan) at 1000, 1600, and 2200 h. A sensor was inserted 1 cm from the anus.

Food intake

Mice were individually housed in ordinary cages, and food intake was assessed by decreases in the weight of chow pellets on hoppers, accounting for spilled crumbs. Mice were acclimated to individual housing for 4 d, and food intake was measured for 3 d. To assess food intake at refeeding after starvation, mice were deprived of food for 48 h from 0900 h and returned to *ad libitum* feeding, and the food intake was measured for 2 h. To see an acute response to ghrelin in food intake, 360 μg/kg of rat ghrelin (Peptide Institute, Osaka, Japan) or saline was sc injected to each mouse at 1100 h on *ad libitum* feeding, and food intake after the injection was measured for 2 h, as described previously (16).

Analyses of mRNA expression

Mice were killed by cervical dislocation at 20 wk of age. Immediately after decapitation, whole hypothalami were dissected out using the fornix and chiasma opticum as landmarks, and interscapular BAT and sc WAT were obtained. Tissues were homogenized by a glass-Teflon homogenizer in a QIAzol reagent (QIAGEN, Hilden, Germany). Total RNA was extracted with an

RNeasy mini kit (QIAGEN), according to the manufacturer's instructions. Total RNA was reverse-transcribed into cDNA using a PrimeScript RT reagent with an oligo deoxythymidine primer (Takara Bio, Otsu, Japan); the reaction was carried out at 42 C for 15 min and terminated by heating at 70 C for 2 min.

CNP and GC-B mRNA expression in tissues was assessed by RT-PCR, in which cDNA corresponding to 50 ng total RNA was used in the PCR step as template. Expression levels of neuropeptide Y (NPY), agouti-related protein (AgRP), proopiomelanocortin (POMC), cocaine- and amphetamine-regulated transcript (CART), melanin-concentrating hormone (MCH), orexin, uncoupling protein (UCP)-1, mitochondrial transcription factor A (mtTFA), peroxisome proliferator-activated receptor (PPAR) γ, PPARγ-coactivator (PGC)-1α, type II iodothyronine deiodinase (D2), muscle-type carnitine palmitoyltransferase (CPT)-1 mRNA were quantified by a real-time RT-PCR with an ABI PRISM 7300 Sequence Detection system (Applied Biosystems, Carlsbad, CA) and a SYBR Premix ExTaq kit (Takara Bio, Otsu, Japan) using a dilution series of the pooled cDNA as the standard. The PCR conditions were the initial denaturation at 95 C for 10 min, followed by 40 cycles of 95 C for 10 sec and 60 C for 32 sec. The mRNA level of each gene was normalized with that of a housekeeping gene, β-actin. Gene-specific primers used are shown in Supplemental Table 1.

Propranolol administration

CNP-Tg/*Nppc*$^{+/+}$ and CNP-Tg/*Nppc*$^{-/-}$ male mice at 20 wk of age were ip injected with propranolol (Sigma, St. Louis, MO) of 20 mg/kg body weight or vehicle (saline) once a day for 3 d, as described in Ref. 17. The interscapular BAT was obtained 2 h after the final injection of propranolol or vehicle, and UCP-1 mRNA expression in the BAT was analyzed, as described above.

Intracerebroventricular injection of CNP

RNA was extracted from the interscapular BAT of C57BL/6J male mice that received a single intracerebroventricular (icv) injection of 10-μg CNP (CNP-22 human, Peptide Institute, Osaka, Japan; dissolved in 2 μl of saline) or vehicle through a 27-gauge microsyringe placed in an appropriate position 4 h before they were killed, as described previously (18). UCP-1, PGC-1α, and D2 mRNA expression in the BAT was analyzed as described above.

Oxygen consumption and locomotor activity

Male mice at 15 wk of age were individually placed in air-tight 15 × 15 × 15 cm plexiglass cages, and oxygen consumption was measured for 24 h by indirect calorimetry with a model MK-5000RQ with an analysis software MMS-2 (Muromachi Kikai, Tokyo, Japan) (19). Spontaneous locomotor activity was measured in a SUPERMEX apparatus with an analysis software CompACT AMS (Muromachi Kikai, Tokyo, Japan) (20). Mice were acclimated to the monitoring for 1 h once a day for 3 d before the 24-h recording.

Statistics

All data are shown as means ± SEM. Statistical differences between two groups and those among more than three groups were assessed by an unpaired *t* test and an ANOVA, respectively. Differences in naso-anal length, body weight, oxygen consumption, and locomotor activity between genotypes were assessed by a repeated measures ANOVA. The level of significance was set at $P < 0.05$.

Results

Growth and metabolic parameters

The growth of male Non-Tg/*Nppc*$^{-/-}$ mice was impaired in both naso-anal length and body weight as compared with male WT (Non-Tg/*Nppc*$^{+/+}$) mice (Fig. 1, A and B), as previously reported (7). The chondrocyte-targeted CNP expression increased the naso-anal length and body weight of male CNP-Tg/*Nppc*$^{-/-}$ mice as compared with those of male Non-Tg/*Nppc*$^{-/-}$ mice (Fig. 1, A and B). The naso-anal length of male CNP-Tg/*Nppc*$^{-/-}$ mice was still significantly less than that of male CNP-Tg/*Nppc*$^{+/+}$ mice, but it surpassed that of male Non-Tg/*Nppc*$^{+/+}$ mice (Fig. 1A). The body weight of male CNP-Tg/*Nppc*$^{-/-}$ mice was significantly reduced as compared with not only that of male CNP-Tg/*Nppc*$^{+/+}$ mice but also that of male Non-Tg/*Nppc*$^{+/+}$ mice (Fig. 1B). At 20 wk of age, the body weight of male CNP-Tg/*Nppc*$^{-/-}$ mice was less than that of male CNP-Tg/*Nppc*$^{+/+}$ mice by 24%. Male CNP-Tg/*Nppc*$^{-/-}$ mice appeared lean and had less abdominal fat as compared with male CNP-Tg/*Nppc*$^{+/+}$ mice (Supplemental Fig. 1, A and B), and epididymal fat pads of male CNP-Tg/*Nppc*$^{-/-}$ mice were less than those of CNP-Tg/*Nppc*$^{+/+}$ mice (Supplemental Fig. 1, C–F). The body fat of male CNP-Tg/*Nppc*$^{-/-}$ mice was significantly less than that of male CNP-Tg/*Nppc*$^{+/+}$ mice: by 50% in absolute values and by 32% in ratios to body weight (Fig. 1, C and D). Upon *ad libitum* feeding, blood glucose, serum insulin, and serum FFA concentrations of CNP-Tg/*Nppc*$^{-/-}$ mice tended to be lower than those of CNP-Tg/*Nppc*$^{+/+}$ mice (Table 1). After overnight fast, blood glucose and serum insulin concentrations decreased in both CNP-Tg/*Nppc*$^{+/+}$ and CNP-Tg/*Nppc*$^{-/-}$ mice, and blood glucose concentrations were significantly lower and serum insulin concentrations tended to be lower in CNP-Tg/*Nppc*$^{-/-}$ mice than those in CNP-Tg/*Nppc*$^{+/+}$ mice (Table 1). After overnight fast, serum FFA concentrations significantly increased in both CNP-Tg/*Nppc*$^{+/+}$ and CNP-Tg/*Nppc*$^{-/-}$ mice, and the increases in CNP-Tg/*Nppc*$^{-/-}$ mice were greater than those in CNP-Tg/*Nppc*$^{+/+}$ mice (Table 1). There were no significant differences in serum free T_4 concentrations between CNP-Tg/*Nppc*$^{+/+}$ and CNP-Tg/*Nppc*$^{-/-}$ mice upon *ad libitum* feeding (Table 1). Serum leptin concentrations in CNP-Tg/*Nppc*$^{-/-}$ mice were about one fifth of those in CNP-Tg/*Nppc*$^{+/+}$ mice upon *ad libitum* feeding (Table 1). Plasma ghrelin concentrations in CNP-Tg/*Nppc*$^{-/-}$ mice tended to be higher than those in CNP-Tg/*Nppc*$^{+/+}$ mice after overnight fast (Table 1).

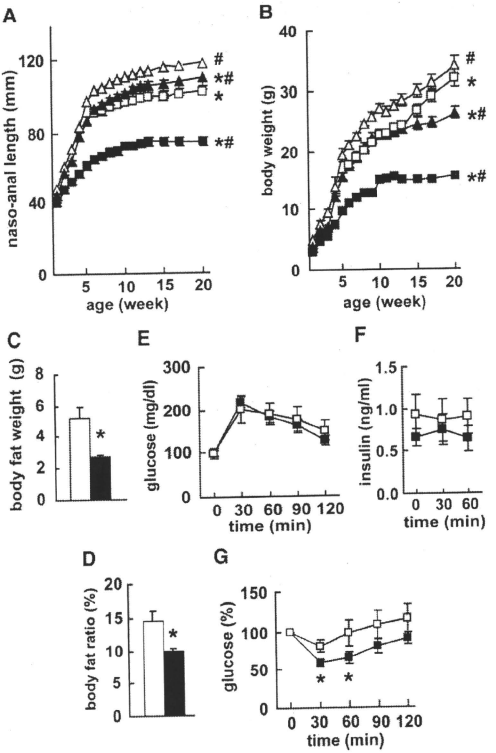

FIG. 1. Growth, body fat accumulation, and glucose and insulin tolerance. A and B, Growth curves of male wild-type (Non-Tg/*Nppc*$^{+/+}$, *open squares*, n = 6), CNP-Tg/*Nppc*$^{+/+}$ (*open triangles*, n = 11), Non-Tg/*Nppc*$^{-/-}$ (*closed squares*, n = 5), and CNP-Tg/*Nppc*$^{-/-}$ (*closed triangles*, n = 7) mice are shown in naso-anal length (A) and body weight (B). *, $P < 0.05$ *vs.* CNP-Tg/*Nppc*$^{+/+}$ mice; #, $P < 0.05$ *vs.* Non-Tg/*Nppc*$^{+/+}$ mice by a repeated measures ANOVA. C and D, The body fat weight of male CNP-Tg/*Nppc*$^{+/+}$ (*open columns*, n = 11) and CNP-Tg/*Nppc*$^{-/-}$ mice (*closed columns*, n = 7) at 20 wk of age are shown in absolute values (C) or ratios to body weight (D). *, $P < 0.05$ *vs.* CNP-Tg/*Nppc*$^{+/+}$ mice by an unpaired *t* test. E and F, GTT in 17-wk-old male mice. Curves of blood glucose (E) and serum insulin concentrations (F) are shown. G, ITT in 17-wk-old male mice. Curves of blood glucose concentrations are shown in percentages to the value before the injection of insulin. In E–G, *open* and *closed squares* represent data of CNP-Tg/*Nppc*$^{+/+}$ (n = 6) and CNP-Tg/*Nppc*$^{-/-}$ mice (n = 14), respectively. *, $P < 0.05$ *vs.* CNP-Tg/*Nppc*$^{+/+}$ mice at each time point by an unpaired *t* test.

Glucose tolerance did not differ between CNP-Tg/*Nppc*$^{+/+}$ and CNP-Tg/*Nppc*$^{-/-}$ mice (Fig. 1E), whereas serum insulin concentrations in CNP-Tg/*Nppc*$^{-/-}$ mice tended to be lower than those in CNP-Tg/*Nppc*$^{+/+}$ mice during the GTT (Fig. 1F). The insulin sensitivity of CNP-Tg/*Nppc*$^{-/-}$ mice assessed by the ITT was significantly better than that of CNP-Tg/*Nppc*$^{+/+}$ mice; decreases of blood glucose levels were 2-fold augmented (Fig. 1G).

Tissue-specific expression of CNP and GC-B mRNA

In CNP-Tg/*Nppc*$^{+/+}$ mice, CNP mRNA was detected in the hypothalamus, but it was not detectable in the interscapular BAT and the sc WAT (Supplemental Fig. 2). This was the case also in WT C57BL/6 mice (data not shown). In CNP-Tg/*Nppc*$^{-/-}$ mice, CNP mRNA was not detectable in these tissues at all (Supplemental Fig. 2). GC-B mRNA was detectable in the hypothalamus, the BAT, and the WAT, and its expression levels were similar among tissues and between CNP-Tg/*Nppc*$^{+/+}$ and CNP-Tg/*Nppc*$^{-/-}$ mice (Supplemental Fig. 2).

Energy expenditure, core body temperature, and sympathetic nervous system activity

The body weight loss during 48-h starvation was significantly greater in male CNP-Tg/*Nppc*$^{-/-}$ mice than that in male CNP-Tg/*Nppc*$^{+/+}$ mice (Fig. 2A). In male CNP-Tg/*Nppc*$^{+/+}$ mice, rectal temperature, which was measured as core body temperature, slightly decreased from 1000 h to 1600 h in the light cycle, and the temperature at 2200 h in the dark cycle was higher than that at 1000 h and 1600 h (Fig. 2B). The diurnal change in rectal temperature appeared to reflect the fact that oxygen consumption and locomotor activity in the dark cycle were greater than those in the light cycle (Fig. 2, C and D). Rectal temperature in CNP-Tg/*Nppc*$^{-/-}$ mice was significantly higher than that in CNP-Tg/*Nppc*$^{+/+}$ mice with the diurnal change being maintained (Fig. 2B). Oxygen consumption in male CNP-Tg/*Nppc*$^{-/-}$ mice was greater than that in male CNP-Tg/*Nppc*$^{+/+}$ mice (Fig. 2C), whereas respiratory quotient did not significantly differ between the genotypes (data not shown). There were no significant differences in locomotor activity between the genotypes (Fig. 2D). At 10–12 wk of age, systolic blood pressure and heart rate tended to be higher, and urinary noradrenalin excretion was significantly greater in male CNP-Tg/*Nppc*$^{-/-}$ mice than those in male CNP-Tg/*Nppc*$^{+/+}$ mice, respectively (Table 1).

TABLE 1. Parameters of metabolism and sympathetic nervous system activity

Genotypes	CNP-Tg/*Nppc*$^{+/+}$ (n = 10)	CNP-Tg/*Nppc*$^{-/-}$ (n = 7)
Blood glucose (mg/dl)		
Ad libitum fed	124 ± 15	92 ± 7
Overnight fast	53 ± 3[b]	42 ± 4[a,b]
Serum insulin (ng/ml)		
Ad libitum fed	3.46 ± 0.76	2.12 ± 0.32
Overnight fast	0.68 ± 0.13[b]	0.39 ± 0.11[b]
Serum FFA (mg/dl)		
Ad libitum fed	0.60 ± 0.05	0.45 ± 0.09
Overnight fast	1.24 ± 0.09[b]	1.30 ± 0.11[b]
Serum free T_4 (ng/dl)		
Ad libitum fed	1.46 ± 0.16	1.28 ± 0.14
Serum leptin (ng/ml)		
Ad libitum fed	9.97 ± 2.12	2.58 ± 0.62[a]
Plasma ghrelin (fmol/ml)		
Overnight fast	36.1 ± 5.7	52.0 ± 7.6
Urinary NA (ng/mgCr)	111 ± 11	142 ± 14[a]
Systolic blood pressure (mm Hg)	95 ± 5	101 ± 5
Heart rate (beat per min)	730 ± 11	756 ± 10

CNP, C-type natriuretic peptide; Tg, transgenic; FFA, free fatty acids; NA, noradrenalin; Cr, creatinine; n, number of mice.

[a] $P < 0.05$ *vs.* CNP-Tg/*Nppc*$^{+/+}$ mice.

[b] $P < 0.05$ *vs. ad libitum* fed in the same genotype.

mRNA expression in BAT

In the interscapular BAT, UCP-1 mRNA levels were significantly higher in CNP-Tg/*Nppc*$^{-/-}$ mice than those in CNP-Tg/*Nppc*$^{+/+}$ mice upon *ad libitum* feeding (Fig. 3A). Levels of mtTFA, PPARγ, PGC-1α, D2, and CPT-1 mRNA in the BAT of CNP-Tg/*Nppc*$^{-/-}$ mice were also significantly higher than those in the BAT of CNP-Tg/*Nppc*$^{+/+}$ mice upon *ad libitum* feeding, respectively (Fig. 3, B–F). The ip injection of propranolol at a dose that did not suppress UCP-1 mRNA levels in the BAT in CNP-Tg/*Nppc*$^{+/+}$ mice significantly suppressed UCP-1 mRNA levels in the BAT in CNP-Tg/*Nppc*$^{-/-}$ mice to levels almost equal to those in the BAT of saline-injected CNP-Tg/*Nppc*$^{+/+}$ mice (Fig. 3G).

The icv injection of CNP to wild-type C57BL/6J male mice failed to suppress UCP-1 mRNA levels in the BAT, but it suppressed PGC-1α and D2 mRNA levels in the BAT, although it did not reach significance, as compared with saline injection (Supplemental Fig. 3).

Food intake

At 14 wk of age, food intake of male CNP-Tg/*Nppc*$^{-/-}$ mice was significantly less by 21% than that of male CNP-Tg/*Nppc*$^{+/+}$ mice (Fig. 4A). When mice were refed after 48-h starvation, food intake of male CNP-Tg/*Nppc*$^{-/-}$ mice was reduced by 61% of that of male CNP-Tg/*Nppc*$^{+/+}$ mice during the first 2 h of refeeding (Fig. 4B). The sc injection of ghrelin augmented food intake in both CNP-Tg/*Nppc*$^{+/+}$ and CNP-Tg/*Nppc*$^{-/-}$ male mice, and increases of food intake were more exaggerated in CNP-Tg/*Nppc*$^{-/-}$ mice than those in CNP-Tg/*Nppc*$^{+/+}$ mice (Fig. 4C).

Expression of mRNA species in hypothalamus

Upon *ad libitum* feeding, mRNA levels of NPY and AgRP in the hypothalamus did not differ between CNP-Tg/*Nppc*$^{+/+}$ and CNP-Tg/*Nppc*$^{-/-}$ mice (Fig. 4, D and E). In hypothalami of both CNP-Tg/*Nppc*$^{+/+}$ and CNP-Tg/*Nppc*$^{-/-}$ mice, NPY and AgRP mRNA levels significantly increased after 48-h fasting as compared with those upon *ad libitum* feeding, and their fold-increases were greater in CNP-Tg/*Nppc*$^{-/-}$ mice than those in CNP-Tg/*Nppc*$^{+/+}$ mice (Fig. 4, D and E). Hypothalamic mRNA levels of POMC, CART, MCH, and orexin were not significantly different between the genotypes either upon *ad libitum* feeding or after the 48-h starvation (data not shown).

Discussion

The chondrocyte-specific CNP expression in CNP-Tg/*Nppc*$^{-/-}$ mice that homozygously harbored the CNP transgene almost completely rescued the dwarf phenotype of *Nppc*$^{-/-}$ mice in naso-anal length (Fig. 1A), which enabled us to investigate roles of CNP in body weight control with minimal influences of skeletal problems in this study. Using Tg mice that homozygously harbor the transgene has a caveat that the transgene might disrupt an unrelated gene, which would participate in the phenotype in which we are interested. Comparisons among mice, all of which homozygously harbor the CNP transgene on C57BL/6 genetic background, can minimize the possibility to take phenotypes due to the disruption of an unrelated gene as those due to the elimination of CNP. Here we showed that the loss of CNP in the whole body except chondrocytes

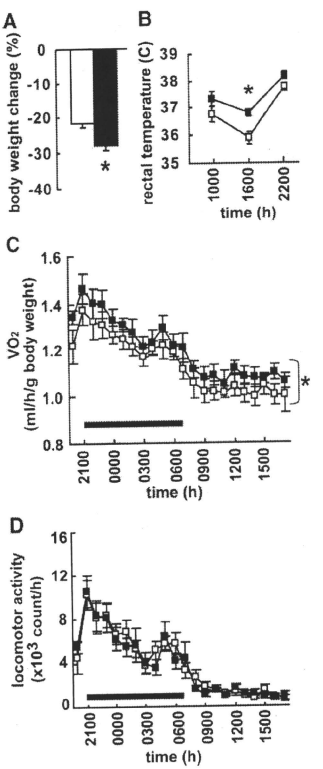

FIG. 2. Parameters of energy expenditure. A, Body weight changes in CNP-Tg/*Nppc*$^{+/+}$ (*open column*, n = 6) and CNP-Tg/*Nppc*$^{-/-}$ mice (*closed column*, n = 6) during 48-h starvation are shown in percentages to body weight before the starvation. *, $P < 0.05$ *vs.* CNP-Tg/*Nppc*$^{+/+}$ mice by an unpaired *t* test. B, Diurnal changes of rectal temperature in CNP-Tg/*Nppc*$^{+/+}$ (*open squares*, n = 14) and CNP-Tg/*Nppc*$^{-/-}$ mice (*closed squares*, n = 7). *, $P < 0.05$ *vs.* CNP-Tg/*Nppc*$^{+/+}$ mice at each time point by an unpaired *t* test. C and D, Oxygen consumption (VO_2, C) and locomotor activity (D) were recorded for 24 h upon *ad libitum* feeding. *Open* and *closed symbols* represent CNP-Tg/*Nppc*$^{+/+}$ (n = 6) and CNP-Tg/*Nppc*$^{-/-}$ mice (n = 6), respectively. A *horizontal black bar* in each panel indicates a dark phase. *, $P < 0.05$ *vs.* CNP-Tg/*Nppc*$^{+/+}$ mice by a repeated measures ANOVA.

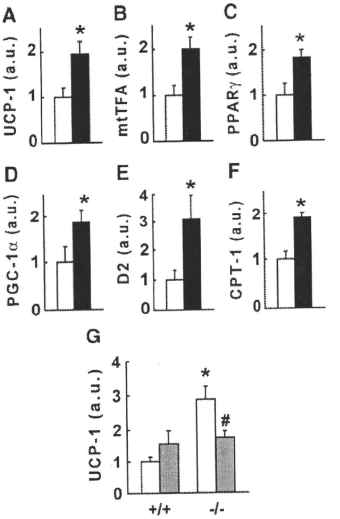

FIG. 3. mRNA expression levels of genes participating in thermogenesis and energy expenditure in brown adipose tissue. Levels of UCP-1 (A), mtTFA (B), PPAR-γ (C), PGC-1α (D), D2 (E), and muscle-type CPT-1 (F) mRNA in CNP-Tg/*Nppc*$^{+/+}$ (*open columns*, n = 6) and CNP-Tg/*Nppc*$^{-/-}$ mice (*closed columns*, n = 6) are shown. Levels of mRNA are normalized with those of mRNA for a house-keeping gene, β-actin. The mean of mRNA levels in CNP-Tg/*Nppc*$^{+/+}$ mice is set as 1.0 arbitrary unit (a.u.). *, $P < 0.05$ *vs.* CNP-Tg/*Nppc*$^{+/+}$ mice by an unpaired *t* test. G, The effect of β-adrenergic blockade by the ip injection of propranolol on UCP-1 mRNA expression in the brown adipose tissue. +/+ and −/− indicate CNP-Tg/*Nppc*$^{+/+}$ and CNP-Tg/*Nppc*$^{-/-}$ mice, respectively. *Open* and *gray columns* represent saline- (n = 4 for each genotype) and propranolol-injected groups (n = 5 for each genotype), respectively. The mean of mRNA levels in the saline-injected group of CNP-Tg/*Nppc*$^{+/+}$ mice is set as 1.0 a.u. *, $P < 0.05$ *vs.* CNP-Tg/*Nppc*$^{+/+}$ mice with the same treatment, #, $P < 0.05$ *vs.* the saline-injected group of the same genotype by an unpaired *t* test.

resulted in reduced body fat accumulation and better insulin sensitivity (Fig. 1, B–G, and Supplemental Fig. 1), indicating that CNP might participate in body fat accumulation and the occurrence of insulin resistance. Two mechanisms could be speculated on how CNP controls energy balance: inhibiting energy expenditure and regulating food intake.

First, we investigated effects of the CNP elimination on energy expenditure. CNP-Tg/*Nppc*$^{-/-}$ mice lost more body weight during 48 h starvation than CNP-Tg/*Nppc*$^{+/+}$ mice (Fig. 2A), indicating that energy expenditure was augmented by the elimination of CNP except chondrocytes. Actually, oxygen consumption in CNP-Tg/*Nppc*$^{-/-}$ mice was greater than that in CNP-Tg/*Nppc*$^{+/+}$ mice (Fig. 2C). The sympathetic nerve input and exogenously administered β-adrenoceptor agonists, including adrenalin and noradrenalin, stimulate thermogenesis in the BAT (reviewed in Ref. 21). FFA and glucose are oxidized in mitochondria to generate proton gradient across the mitochondrial inner membrane, which is used to synthesize ATP by F0/F1-ATPase (21). β-Adrenoceptor stimulation increases the mRNA expression of UCP-1, which

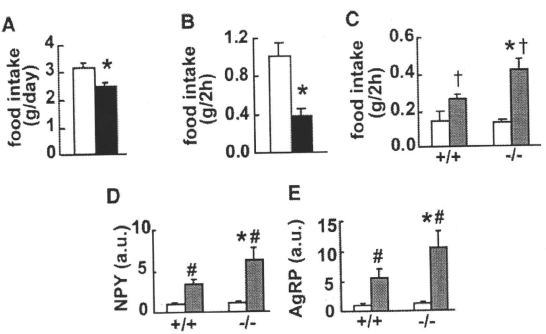

FIG. 4. Food intake and hypothalamic mRNA expression. A, Food intake of male mice at 17 wk of age upon *ad libitum* feeding is shown in absolute values. B, Food intake of male mice at 17 wk of age during the first 2 h at refeeding after 48-h starvation is shown in absolute values. In A and B, *open* and *closed columns* represent data of CNP-Tg/*Nppc*$^{+/+}$ (n = 6) and CNP-Tg/*Nppc*$^{-/-}$ mice (n = 6), respectively. *, $P < 0.05$ *vs.* CNP-Tg/*Nppc*$^{+/+}$ mice by an unpaired *t* test. C, Response in food intake to sc injection of ghrelin at 360 μg/kg body weight or saline. Food intake during the first 2 h after the injection is shown in absolute values. *Open* and *gray columns* represent data of saline (n = 8) and ghrelin groups (n = 8), respectively. +/+ and −/− indicate CNP-Tg/*Nppc*$^{+/+}$ and CNP-Tg/*Nppc*$^{-/-}$ mice, respectively, in panels C–E. *, $P < 0.05$ *vs.* +/+ in each treatment group; †, $P < 0.05$ *vs.* the saline group in each genotype by an ANOVA. D and E, mRNA expression levels of NPY (D) and AgRP (E) in the hypothalamus upon *ad libitum* feeding (*open columns*; +/+, n = 10; −/−, n = 10) and after 48-h starvation (*gray columns*; +/+, n = 10; −/−, n = 8). Expression levels of mRNA are normalized with those of a house-keeping gene, β-actin. The mean of mRNA expression levels in +/+ upon *ad libitum* feeding is set 1.0 arbitrary unit (a.u.). *, $P < 0.05$ *vs.* +/+ at each feeding status; #, $P < 0.05$ *vs. ad libitum* feeding at each genotype by an ANOVA.

causes proton leak back across the mitochondrial inner membrane and generates heat, in the BAT by two molecules: PGC-1α and D2 (21). The increase of the intracellular cAMP concentration augments the mRNA expression of PGC-1α and D2. PGC-1α coactivates the UCP-1 gene transcription with transcription factors, such as PPARγ and T_3-bound thyroid hormone receptor, and D2 converts T_4 to T_3 and increases T_3-bound thyroid hormone receptors (21). PGC-1α also coactivates the gene transcription of transcription factors, which positively regulate mitochondrial biogenesis, such as mtTFA (21). The protein kinase A pathway that is activated by cAMP stimulates lipolysis via the activation of hormone-sensitive lipase and increases FFAs, which activate UCP-1 protein (21). FFAs stimulate the gene transcription of the muscle-type CPT-1 via PPARγ and α and enhance β-oxidation of FFAs (22). The muscle-type CPT-1 is a key regulator of β-oxidation in skeletal and cardiac muscles and the BAT (23). In CNP-Tg/*Nppc*$^{-/-}$ mice, CNP mRNA was not aberrantly expressed in the BAT (Supplemental Fig. 2), which enabled us to investigate effects of the CNP elimination in the BAT in this study. The elimination of CNP except chondrocytes elevated UCP-1 and mtTFA mRNA levels in the BAT (Fig. 3, A and B). It also augmented the mRNA expression of PPARγ, PGC-1α, D2, and CPT-1, which consist of the machinery that augments the gene transcription of UCP-1 and mtTFA or activates UCP-1 protein downstream to the β-adrenoceptor/cAMP cascade (Fig. 3, C–F). Because locomotor activity was similar between CNP-Tg/*Nppc*$^{+/+}$ and CNP-Tg/*Nppc*$^{-/-}$ mice (Fig. 2D), it is unlikely that energy expenditure was augmented by locomotor activity. Taken together with the observation that core body temperature in CNP-Tg/*Nppc*$^{-/-}$ mice was elevated over that in CNP-Tg/*Nppc*$^{+/+}$ mice (Fig. 2B), it is suggested that the elimination of CNP except chondrocytes augmented energy expenditure by thermogenesis via the generation and activation of the UCP-1 and the augmentation of mitochondrial biogenesis.

Our observation that urinary noradrenalin excretion in CNP-Tg/*Nppc*$^{-/-}$ mice was higher than that in CNP-Tg/*Nppc*$^{+/+}$ mice (Table 1) suggests that the SNS activity was augmented in CNP-Tg/*Nppc*$^{-/-}$ mice as compared with that in CNP-Tg/*Nppc*$^{+/+}$ mice. It was also reported that the SNS activity was augmented in Tg rats expressing a dominant-negative mutant of GC-B, which inhibited the CNP-dependent activation of authentic GC-B, where the activity was assessed by heart rate and the low-frequency/high-frequency ratio in Fourier transformation of pulse intervals (24). Because the ip administration of propranolol, a nonselective β-adrenoceptor blocking agent, could cancel the augmentation of UCP-1 mRNA expression in the BAT of CNP-Tg/*Nppc*$^{-/-}$ mice (Fig. 3G), the site of CNP action on energy expenditure appears to be located within or upstream to the SNS. In rodents, the SNS governs thermogenesis in the BAT, under the control of neurons in the paraventricular nucleus of the hypothalamus (25) where both CNP and GC-B are expressed (13, 14). It was also reported that neurons that inhibit the SNS activity and thermogenesis in the BAT were present in the preoptic area (26), in which CNP mRNA was abundantly detected (27). In mice, GC-B mRNA could be detected in both the hypothalamus and the BAT, but CNP mRNA was detectable only in the hypothalamus (Supplemental Fig. 2). Considering the nature of CNP as a local regulator (1), a site of CNP actions may be the hypothalamus. In wild-type C57BL/6J mice, the icv administration of CNP tended to

suppress mRNA levels of PGC-1α and D2, which synergistically activate UCP-1 transcription downstream to the β-adrenoceptor/cAMP cascade stimulated by the SNS (21), in the BAT (Supplemental Fig. 3). Taken together, CNP appears to centrally inhibit the SNS activity and thermogenesis in the BAT, although further analyses will be needed to see the precise cite of CNP actions.

It was reported that atrial natriuretic peptide, which is another member of the natriuretic peptide family and increases intracellular cGMP concentrations via GC-A as CNP does via GC-B, could decrease circulating T_4 and T_3 concentrations via a direct action on the thyroid (28). If this is also true for CNP, the elimination of CNP might increase serum T_4 and T_3 concentrations. Because thyroid hormone is a major regulator of mitochondrial biogenesis and thermogenesis (21), an increase of serum thyroid hormone levels can augment thermogenesis and energy expenditure. However, there were no significant differences in serum free T_4 concentrations between CNP-Tg/*Nppc*$^{+/+}$ and CNP-Tg/*Nppc*$^{-/-}$ mice (Table 1).

Next, we investigated effects of the CNP elimination on food intake. Food intake of CNP-Tg/*Nppc*$^{-/-}$ mice was less than that of CNP-Tg/*Nppc*$^{+/+}$ mice upon *ad libitum* feeding (Fig. 4A), and the 48-h starvation stimulated food intake much less in CNP-Tg/*Nppc*$^{-/-}$ mice than it did in CNP-Tg/*Nppc*$^{+/+}$ mice (Fig. 4B), indicating that CNP might participate in the control of food intake. Neuropeptides expressed in the ARC of the hypothalamus play important roles to control food intake (12). NPY and AgRP expressed in neurons of the ARC stimulate MCH and orexin neurons in the lateral hypothalamic area and increase food intake (reviewed in Ref. 12). POMC and CART expressed in other neurons of the ARC inhibit MCH and orexin neurons in the lateral hypothalamic area and decrease food intake (12). It was shown that CNP mRNA is abundantly expressed in the ARC of the hypothalamus (13). We, therefore, analyzed mRNA expression of these peptides in the hypothalamus. CNP mRNA expression in the hypothalamus was neither impaired in CNP-Tg/*Nppc*$^{+/+}$ mice nor aberrantly induced in CNP-Tg/*Nppc*$^{-/-}$ mice by the presence of the transgene (Supplemental Fig. 2). In hypothalami of CNP-Tg/*Nppc*$^{-/-}$ mice, increases of NPY and AgRP mRNA levels upon starvation were augmented (Fig. 4, D and E) and mRNA expression of POMC, CART, MCH, and orexin was not deteriorated (data not shown), as compared with those in hypothalami of CNP-Tg/*Nppc*$^{+/+}$ mice. Based on these data, we can speculate that there might be AgRP/NPY resistance in CNP-Tg/*Nppc*$^{-/-}$ mice. If CNP is indispensable for the generation or function of a system that links the activation of AgRP/NPY neurons with feeding behavior, the activation of AgRP/NPY neurons cannot increase food intake in the absence of CNP from the beginning of life. It was reported that CNP/GC-B signaling might be important for perinatal brain maturation (29). In another report, it was suggested that the CNP/GC-B system enhances the maturation of olfactory receptor neurons (30). Although we have not yet identified any apparent anatomical abnormalities in the brain (data not shown), there might be functional problems in the neuronal circuit regulating food intake in CNP-Tg/*Nppc*$^{-/-}$ mice. Although skeletal problems were minimized in our CNP-Tg/*Nppc*$^{-/-}$ mice, we cannot completely exclude the possibility that food intake is influenced by minimal skeletal differences between CNP-Tg/*Nppc*$^{-/-}$ and CNP-Tg/*Nppc*$^{+/+}$ mice.

Ghrelin, which was isolated as an endogenous ligand for the growth-hormone secretagogue receptor, is a peptide secreted from the gastric mucosa and stimulates appetite via direct actions on the hypothalamus or signals through the vagal afferent (31–33). Increases of food intake by ghrelin injected sc in CNP-Tg/*Nppc*$^{-/-}$ mice were greater than those in CNP-Tg/*Nppc*$^{+/+}$ mice (Fig. 4C). This observation indicates that CNP might inhibit ghrelin signaling that augments food intake. This suggests that a physiological action of CNP would be the inhibition of food intake, which does not support our observation that CNP-Tg/*Nppc*$^{-/-}$ mice took less food than CNP-Tg/*Nppc*$^{+/+}$ mice (Fig. 4, A and B). We, therefore, cannot simply conclude that CNP physiologically stimulates food intake.

NPY potently stimulates food intake, at least in part, through the NPY Y5 receptor (reviewed in Ref. 12). In Y5 receptor-null mice, however, food intake, body weight, and total fat pad weight were greater than those in WT mice (34). Five NPY receptors have been identified in mice and play roles different from each other in the regulation of physiological functions such as food intake (35). The complexity of the receptor system might be a cause of the difficult-to-understand phenotype of the Y5-null mice. CNP also has a complicated receptor system. Three GC-B isoforms are generated from the single GC-B gene by alternative splicing in mice: GC-B1, which is the authentic GC-B that increases GC activity upon CNP binding, and two dominant-negative isoforms of GC-B (GC-B2 and GC-B3) (10). The brain is demonstrated to be an organ that expresses mRNA of GC-B2, which has the basal GC activity as GC-B1 does, lacks the CNP-dependent increase of the GC activity, and interferes with the CNP-dependent increase of the GC activity of GC-B1, at a high level (10). Elucidating the nucleus- or cell-specific expression of CNP and GC-B isoforms in the brain would help us understand precise mechanisms of how the CNP/GC-B system controls food intake and energy expenditure.